2015

Morphological and Surface Chemistry Characteristics of Silica Nanoparticle Based Cryogels from Specific Processing Parameters

Ben Walusiak
Eastern Illinois University

The Graduate School
EASTERN ILLINOIS UNIVERSITY

Thesis Maintenance and Reproduction Certificate

FOR: Graduate Candidates Completing Theses in Partial Fulfillment of the Degree
Graduate Faculty Advisors Directing the Theses

RE: Preservation, Reproduction, and Distribution of Thesis Research

---

Preserving, reproducing, and distributing thesis research is an important part of Booth Library's responsibility to provide access to scholarship. In order to further this goal, Booth Library makes all graduate theses completed as part of a degree program at Eastern Illinois University available for personal study, research, and other not-for-profit educational purposes. Under 17 U.S.C. § 108, the library may reproduce and distribute a copy without infringing on copyright; however, professional courtesy dictates that permission be requested from the author before doing so.

Your signatures affirm the following:

- The graduate candidate is the author of this thesis.
- The graduate candidate retains the copyright and intellectual property rights associated with the original research, creative activity, and intellectual or artistic content of the thesis.
- The graduate candidate certifies her/his compliance with federal copyright law (Title 17 of the U. S. Code) and her/his right to authorize reproduction and distribution of all copyrighted materials included in this thesis.
- The graduate candidate in consultation with the faculty advisor grants Booth Library the non-exclusive, perpetual right to make copies of the thesis freely and publicly available without restriction, by means of any current or successive technology, including by not limited to photocopying, microfilm, digitization, or internet.
- The graduate candidate acknowledges that by depositing her/his thesis with Booth Library, her/his work is available for viewing by the public and may be borrowed through the library's circulation and interlibrary loan departments, or accessed electronically.
- The graduate candidate waives the confidentiality provisions of the Family Educational Rights and Privacy Act (FERPA) (20 U. S. C. § 1232g; 34 CFR Part 99) with respect to the contents of the thesis and with respect to information concerning authorship of the thesis, including name and status as a student at Eastern Illinois University.

I have conferred with my graduate faculty advisor. My signature below indicates that I have read and agree with the above statements, and hereby give my permission to allow Booth Library to reproduce and distribute my thesis. My adviser's signature indicates concurrence to reproduce and distribute the thesis.

Graduate Candidate Signature

Faculty Adviser Signature

Printed Name

Printed Name

Graduate Degree Program

Date

Please submit in duplicate.

Morphological and Surface Chemistry Characteristics of Silica

Nanoparticle Based Cryogels from Specific Processing Parameters

(TITLE)

BY

Ben Walusiak

THESIS

SUBMITTED IN PARTIAL FULFILLMENT OF THE REQUIREMENTS
FOR THE DEGREE OF

Master of Science in Chemistry

IN THE GRADUATE SCHOOL, EASTERN ILLINOIS UNIVERSITY
CHARLESTON, ILLINOIS

2015

YEAR

I HEREBY RECOMMEND THAT THIS THESIS BE ACCEPTED AS FULFILLING
THIS PART OF THE GRADUATE DEGREE CITED ABOVE

THESIS COMMITTEE CHAIR DATE	DEPARTMENT/SCHOOL CHAIR OR CHAIR'S DESIGNEE DATE
THESIS COMMITTEE MEMBER DATE	THESIS COMMITTEE MEMBER DATE
THESIS COMMITTEE MEMBER DATE	THESIS COMMITTEE MEMBER DATE

Contents

Figures

Tables

Abstract

The goal of this research was to determine the effects of processing conditions on the morphology and surface chemistry of silica nanoparticle based cryogels. All processing conditions resulted in a change in morphology or surface chemistry compared to the starting material, CAB-O-SIL HS5 fumed silica. N_2 adsorption isotherms were used to characterize surface area and pore size distributions of fumed silica and silica cryogels. TGA (thermogravimetric analysis) was performed on all samples in order to characterize the adsorbed water and hydroxyl group content of the silica surface. Solid state ^{29}Si NMR was also used to evaluate surface chemistry of the cryogel samples. It was found that exposure of the silica surface to excess water during cryogel preparation results in a higher degree of hydroxylation than the bare, unprocessed silica. Freezing and freeze drying most prominently affect the morphological properties of the cryogel, such as bulk density and pore volume. Freeze drying can cause a high degree of variability in both bulk density and pore volume, which can override smaller effects on cryogel morphology caused by other processing parameters. The surface of silica heated to 650°C before cryogel processing was largely de-hydroxylated, and did not fully re-hydroxylate in the presence of water. When exposed to high pH (10) conditions, the surface area of a silica cryogel is reduced due to the increased solubility of silica in water at high pH. Overall, cryogel processing parameters result in significant changes from the starting material. Many processing parameters result in morphological changes, although surface chemistry has been shown to play an important role in determining the properties of all cryogel samples.

Introduction

Silica or silicon dioxide (SiO_2) is an especially common material, making up the bulk of common, everyday materials such as glass, gemstones such as quartz or agate, and is one of the most common materials in the Earth's crust. Pure silica varies widely in form, from monolithic crystals to powders. Forms of silica can be divided into the following groups:[1]

1. Anhydrous crystalline SiO_2.
2. Hydrated crystalline silica $SiO_2 \cdot xH_2O$.
3. Anhydrous amorphous silica of microporous anisotropic form such as fibers or sheets.
4. Anhydrous and hydrous amorphous silica of colloidally subdivided or microporous isotropic form such as sols, gels, and fine powders.
5. Massive dense amorphous silica glass

This thesis deals with silica form number 4, specifically the morphology and surface chemistry of cryogels manufactured from nanoparticulate fumed silica slurries.

In its pure form, silica can assume a wide range of crystalline forms such as quartz and tridymite, as well as several amorphous varieties. Silica (or any other element/compound) can be referred to as crystalline if it can be seen to have long term order in its crystal structure. That is to say that by knowing the position of one atom in the crystal lattice, one can predict the locations of all other atoms in the crystal lattice, assuming a perfect arrangement with no defects. Amorphous silica has only short term order to the crystal structure, meaning the specific arrangement of silicon and oxygen atoms is not well defined beyond the first few nearest neighbor atoms. Silicas of all types are used in a huge variety of industrial processes. Silica sand is used as a raw material for manufacturing everyday glass, while purer forms of silica are used

for more sensitive and specialized applications such as fiber optics. In fact, the manufacture of extremely pure silica for the express purpose of making fiber optic cables is possible only with a bit of help from the electronics industry, which can provide extremely pure silicon as a raw material.[2] Silica gel is an amorphous and porous form of silica with quite a high surface area, enabling it to effectively adsorb water from the atmosphere and act as a desiccant. Micron sized spherical silica particles can even be used as a chromatographic column packing. A column packed with silica can serve as either a microporous sieve through which larger molecules diffuse more slowly, or as a type of affinity column, where various analyte components adhere to the surface of the silica with varying degrees of strength.[1]

Fumed silica, the type of silica used in this study, has an amorphous structure, which is in part due to the method in which it is manufactured. The fumed silica is produced by burning silicon tetrachloride in a flame of hydrogen and oxygen at about 1800°C[3]. This production process causes the resulting silica to assume an amorphous phase, akin to glass and unlike crystalline quartz. The amorphous structure results in a silica with a lower density (~2.2 g/cm^3) than its crystalline counterpart (2.65 g/cm^3). Fumed silicas, specifically those produced by the Cabot Corporation, are sold under the brand name CAB-O-SIL, typically exhibit a surface area of ~160-380 m^2/g. CAB-O-SIL HS5 was the specific type used in this study, which was not processed beyond its initial production, as Cabot fumed silicas sometimes are.[4] Amorphous silicas, especially in the form of fine particles (micro or nano-sized), are actually more reactive than crystalline silica, and as such are able to be fused together at lower temperature and manipulated in a variety of reactions, such as conversion to silicon nitride (Si_3N_4), at a lower temperature than crystalline silica.[1]

One area of interest in the study of silica is the effect of surface chemistry on the behavior and properties of the solid silica particles. When the silica lattice terminates, the atoms at the terminus, deprived of their preferred number of nearest neighbors, exhibit residual valences or charges as a result. The presence of the oxygen and silicon atoms on the surface not only permits them to react physically with their surroundings, but chemically as well. For example, not only can water molecules interact via hydrogen bonding with the surface, but all silica that is exposed to water and dried below the point of 150°C contains surface SiOH groups.[1] More specifically, a silica surface that has been exposed to excess water and dried at any temperature below 150°C will contain a number of SiOH groups, which has been shown to have a maximum value of 4.6 to 4.9 OH groups per square nanometer.[5] There are two forms of SiOH groups that can exist on the silica surface: hydroxyl groups that are hydrogen bonded to one another, and the non-hydrogen bonded hydroxyl groups that do not interact with other hydroxyl groups. A diagram of this can be seen below in Figure 1. Also present on the silica surface are siloxane (Si-O-Si) groups, also pictured in Figure 1. Just as interaction with water

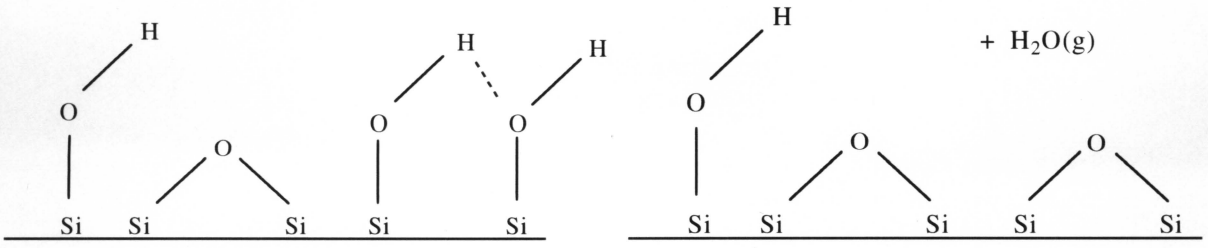

Figure 1. Non-hydrogen bonded hydroxyl grup, siloxane group, hydrogen bonded hydroxyl groups (left). Non-hydrogen bonded hydroxyl group and two siloxane groups (right).

can cause the formation of hydroxyl groups on silica surfaces, these hydroxyl groups can also be driven from the surface by simply heating the sample. Previous literature indicates that three temperature regimes exist for the removal of water and/or hydroxyl groups from the surface of silica. In the 100-200°C range, water molecules interacting with the surface of the silica are

driven off.[6] Hydrogen bonding interactions with the silica surface prevent the water molecules from simply leaving en masse at exactly 100°C. From 200-600°C the hydrogen bonded hydroxyl groups are driven off in the form of water via a condensation reaction. Finally, from 600-800°C a portion of the non-hydrogen bonded hydroxyl groups are driven from the surface of the silica. The reason that the hydrogen bonded hydroxyl groups can be removed from the surface at a lower temperature than the non-hydrogen bonded hydroxyl groups is that two hydroxyl groups near each other (hydrogen bonded) can more easily form a water molecule and escape the surface (Figure 1). In the same fashion, weakly interacting hydroxyl groups, such as those at an intermediate distance from one another, are driven off after closely interacting hydroxyl groups, but still before the non-hydrogen bonded hydroxyl groups. As will be explained later, the surface properties of amorphous silica depend largely on the presence of surface silanol groups.[5] Hydroxyl group concentration can affect properties of the silica material as a whole, such as optical transparency. For example, transparency in the 1400 nm region of the electromagnetic spectrum (infrared) can be increased by limiting the number of hydroxyl groups present, while in contrast a high number of surface hydroxyl groups will actually increase transparency of the silica in the UV region.[2]

Cryogelation and Surface Chemistry

This study focuses on the concept of a supposed cryogelation mechanism upon freezing an aqueous silica slurry. In general, cryogelation is characterized by the formation of polymeric, protein, solid or composite gels under cryogenic treatment; which is to say freezing an initial solution or suspension and keeping it frozen for a certain period of time, which results in pore formation and physical or chemical cross-linking of the compounds involved. Formation of ice crystallites upon freezing of the bulk liquid pushes the non-bulk material aside, effectively

trapping and compressing it between the ice crystallites. This mechanism results in the formation of a porous network of solute material as detailed in Fig. 2 After the solute molecules/particles are forced together by the freezing action, they react or interact in some fashion to form a permanent or semi-permanent structure. Chemical bonds, temporary interactions, or physical interactions may all occur. The frozen bulk material is then removed by simple evaporation or by lyophilization, leaving the porous network intact. A completed cryogel need not be one monolithic piece, but can take the form of clumps of secondary, tertiary, etc. structures, which may result in a powder like texture.

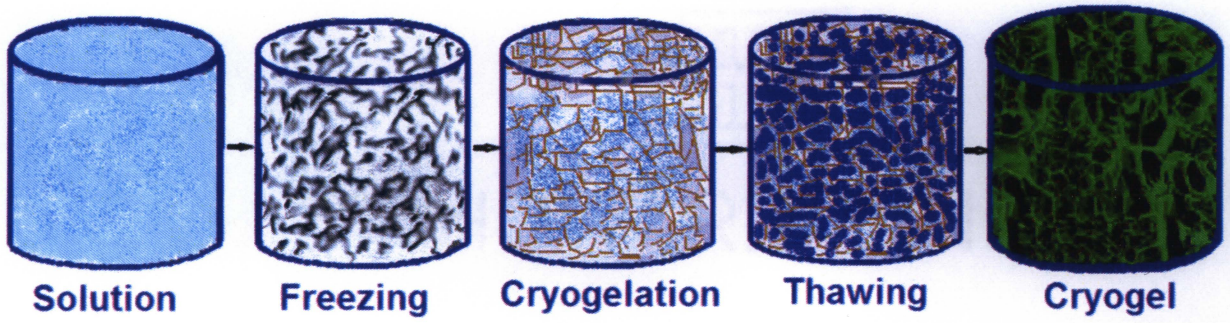

Figure 2. Cryogel preparation stages: (i) a solution or suspension of reactive monomers or bulk particles, (ii) frozen mixture, (iii) stored at subzero temperature, and (iv) thawed to form (v) macroporous cryogel in native hydration state (which can then be freeze dried).[7]

Conventions for describing pore sizes in silica cryogels and other porous materials have been previously described.[7] Different classes of pores are described as follows: *nanopores* have a radius of $R < 1$ nm, *mesopores* have radius of $1 < R < 25$ nm, and *macropores* have a radius of $R > 25$ nm. Cryogels of all kinds have a myriad of potential uses. As a class of materials, cryogels are mainly macroporous materials, and they can be thought of as useful matrices that allow unhindered diffusion not only of low-molecular weight dissolved compounds but also macromolecules, cells, *etc.* due to the interconnected systems of macropores.[7] The cryogel

surface may be further modified, chemically or physically, to affect its interaction with the environment. For example, adsorption of various polymers or ligands to the cryogel surface may enable the system to trap or modify compounds that come into contact with the modified surface.

Previous work on cryogels largely seeks to characterize their physical properties or adapt these materials for a variety of applications. An example of one type of inorganic oxide cryogel synthesis involves freezing silicon dioxide nanoparticles under varying pressures and examining their morphological and surface characteristics. Work by Gun'ko et al.[8] found that the properties of these cryogels, such as adsorption of water and other co-adsorbates, can vary depending on temperature, silica concentration, and dispersion medium. The interfacial behavior of adsorbates was measured via low temperature NMR spectroscopy.[8] In the aforementioned experiment, cryogels take the form of a powder, made up of aggregates and agglomerates of spherical particles. Other experiments utilize cryogelation to impart a specific morphology to the final material. This is done by freezing a sol gel precursor, rather than manipulating metal oxide particles created previously. A 2010 paper by Nishihara et al.[9] describes unidirectional freezing of a composite silica titania hydrogel, which results in the formation of a honeycomb type structure in the final, dried material. This honeycomb type structure serves to increase the surface area of the material, and is achieved by controlling the mobility of the titania-silica hydrogel precursor (the sample mixture before freezing and freeze drying). The titania was included to utilize its photocatalytic properties to break down salad oil.[9] Cryogel materials may also be used for applications such as energy storage. A 2012 paper in the Journal of Physical Chemistry by Wang et al.[10] describes the performance of a hierarchal Co_3O_4 meso and macroporous network for use in a supercapacitor electrode. Like the Nishihara paper, a sol-gel precursor was prepared, which was then further processed via a freeze drying method in order to obtain the final

product.[10] Previous research has recognized the potential of cryogelation processes, especially freezing and freeze drying, to control the final morphology of certain materials. This study seeks to further understand the factors that influence the properties of SiO_2 derived cryogels.

An important step in understanding silica based cryogels is to take into account the surface chemistry of the silica itself. Whether during synthesis or upon exposure to water, Si-OH groups are almost always formed to some extent on the surface of silica.[1] The amount and nature of surface hydroxyl groups on silica are of interest because of their ability to react with various compounds and chemisorb, or attach by chemical reaction, these compounds onto the surface. An example reaction is given below in which a bond is formed[1] between the Si atom on the surface and an atom of an external compound.

$$Si_sOH + ROH = Si_sOR + H_2O$$

Though reactions can occur on a non-hydroxylated silica surface, with a siloxane group for example, the great majority of possible surface reactions explored in previous literature involve a surface SiOH group at the start of each reaction.[1] SiOH groups also interact with surrounding molecules, such as water, via hydrogen bonding. This interaction is an important component of the behavior of nanoparticulate silica, especially in aqueous systems.

Analytical Techniques for Probing Surface Chemistry and Morphology

IR

The quantity and specific properties of surface bound SiOH groups can be probed by several methods, including thermogravimetric analysis, infrared (IR) spectroscopy, and nuclear magnetic resonance (NMR). Below in Figure 3 one can see a series of reflectance IR spectra

taken from an unmodified silica gel at varying temperatures. Reflectance IR analysis is a method, described in the literature, in which the IR beam is not transmitted through the sample, but instead is reflected off of the sample surface, possibly yielding more sensitive information (compared to transmittance IR) about surface species, whether adsorbed or chemically attached.[11] Figure 3 shows a series of overlaid IR spectra with each curve representing a spectrum taken at a different temperature. The top most curve indicates a spectrum taken at

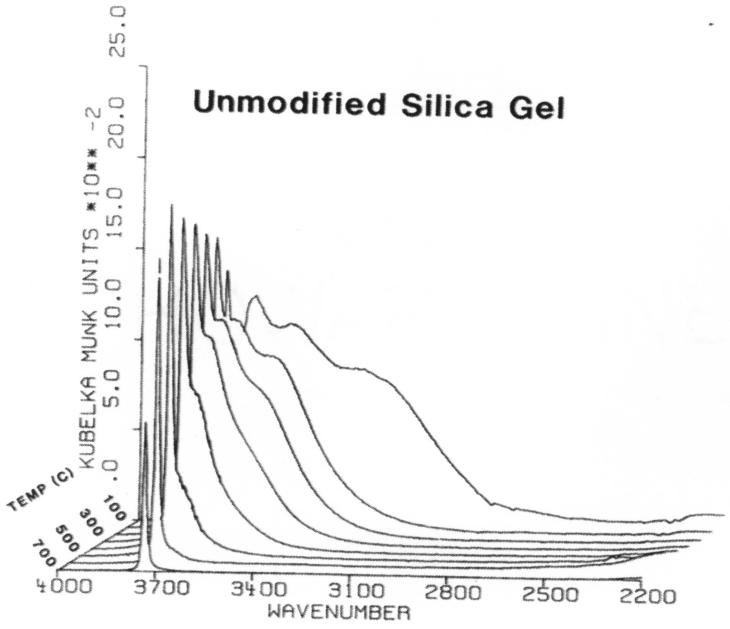

Figure 3. A series of overlayed IR spectra of unmodified silica showing the removal of hydrogen bonded hydroxyl groups (~3100 cm-1) upon heating as well as the removal of non-hydrogen bonded hydroxyl groups (~3650 cm-1) upon further heating.[6]

100°C and each subsequent curve, moving closer to the x axis, represents a spectrum taken at a higher temperature, all the way up to 700°C. The diffuse peak centered on ~3100 cm^{-1} represents the hydrogen bonded hydroxyl groups, which are able to condense as water relatively easily and be driven from the silica surface. The hydrogen bonded hydroxyl peak thus diminishes very quickly leaving behind the peak centered on ~3650 cm^{-1}, resulting from the non-hydrogen bonded hydroxyl groups. As one can see from the graph, this peak does not start diminishing

appreciably until 700°C, which is in line with previous literature.[12] One can see how such data would be relevant and illuminating regarding the relative quantity and type (hydrogen bonded vs. non-hydrogen bonded) of hydroxyl groups.

Bulk Density

A property of interest for many materials, in powder form especially, is bulk density. In addition to affecting the handling of the bulk material, bulk density is indicative of the grouping of small primary particles that make up the powder itself.[13] The primary particles can come together to form primary structures, referred to as aggregation, and these in turn can clump together to from agglomerates. The exact nature of the primary, secondary, tertiary structure of such materials, like oxide based cryogels, is influenced by many factors. However, a high bulk density generally indicates a closer interaction of the primary particles. When combined with other analytical techniques, simple bulk density measurements can contribute to the understanding of the sample morphology and even surface chemistry. One can take advantage of the particular surface chemistry of silica to aid in this regard.

TGA

Another method of probing the surface chemistry of nanoparticulate silica is known as thermogravimetric analysis (TGA). As stated above, free water and hydroxyl groups are driven from the silica surface in three temperature ranges 100-200°C, 200-600°C and 600-800°C.[12] As mentioned above, these temperature ranges correspond to: the evacuation of surface water, hydroxyl groups hydrogen bonded with another hydroxyl group, and a portion of the non-hydrogen bonded hydroxyl groups, respectively. Thermogravimetric analysis incorporates a sensitive microbalance into a furnace assembly for the purpose of precisely measuring weight loss, down to fractions of a milligram, as a function of temperature.[14] By knowing the sample

weight and the amount of material lost in each temperature range, one can quantify the amount of free water and hydroxyl groups of both types present in a certain amount of sample. Different processing parameters such as initial particle size, silica slurry concentration, freezing temperature, or pressure can potentially combine in many ways to affect sample morphology, and other parameters. Previous studies have shown that the initial silica-water concentration, pressure, and compaction during freezing can affect at least the amount of water (not hydroxyl groups) that desorbs from a cryogel sample.[12] This means that parameters such as freezing and pressure during freezing can affect the morphology, which includes the pore structure, of a cryogel, which can in turn influence how a silica surface can retain water.[12] The specific physical environment, inside a pore for example, affects the interaction between the silica surface and the adsorbed water. This has also been shown to affect how other chemicals interact with the surface as well.[1,12] TGA can be quite useful when comparing samples that may have been altered by heating, chemical changes, or other sample processing parameters. However, thermogravimetric analysis is not capable of determining minute, quantitative parameters such as the specific concentration of surface hydroxyl groups. It is more suitable to point out general differences between samples.

N_2 Adsorption

N_2 adsorption/desorption analysis can be used to determine the surface area and overall pore structure of nanoparticulate silica and virtually any other solid material of interest. One of the more common methods used to obtain useful information from N_2 adsorption desorption experiments is the BET (named for Brunauer, Emmett, Teller) method.[15] Essentially, the surface area of a material can be measured by covering the surface with a monolayer of N_2 molecules, and since the area covered by a nitrogen molecule is known[1] (16.2Å^2), the surface area can then

be calculated as explained below. Performed at 77K, the temperature of liquid nitrogen, precise measurement of the partial pressure of nitrogen and subsequent analysis using equation 1 yields the volume of nitrogen adsorbed and thus the specific surface area of the material.[1] In equation 1 p is the gas pressure,

$$\frac{p}{v_a(p_o-p)} = \frac{1}{v_m c} + \frac{(c-1)p}{v_m c p_o} \quad (1)$$

v_a is moles of gas adsorbed per gram of adsorbent material, v_m is the monolayer capacity of the surface, p_o is the saturation gas pressure at the temperature used in the experiment, and c is a constant defined in equation 2 below. c is simply a constant where E_1 is the heat of

$$c = \frac{(E_1-E_L)}{RT} \quad (2)$$

adsorption for the first monolayer on the surface, E_L is the heat of adsorption for the second and all subsequent adsorption layers.[16] Equation 1, otherwise known as an adsorption isotherm, can be plotted in order to determine the specific surface area of the sample. A plot of $\frac{p}{v_a(p_o-p)}$ as the y axis and with $\frac{p}{p_o}$ as the x axis yields a line with slope A and y intercept I.[16] Equations 3 and 4

$$v_m = \frac{1}{A+I} \quad (3)$$

$$c = 1 + \frac{A}{I} \quad (4)$$

$$S_{BET} = v_m a_m N \cdot 10^{-20} \quad (5)$$

yield v_m and c, while equation 5 gives S_{BET}, the specific surface area of the sample in m^2/g.[1] N is Avogadro's number and a_m is the cross-sectional area of one nitrogen molecule in $Å^2$ (16.2). N_2

adsorption can also be used to calculate the pore size and pore size distribution[12,15] of porous samples. However, nitrogen as used in N_2 adsorption studies can only efficiently fill pores up to 40 nm, which is ideal for the 3 categories of pores described above.[15] The volume of pores with r >40 nm can be calculated using the bulk density and the volume of pores with r <40 nm[12]. Many parameters, such as pressure and slurry concentration, can affect the size and distribution of pores[12] in cryogel samples. Therefore an important part of any analysis of cryogel materials would be the characterization of the pore size, since pore size and pore size distribution can dictate the properties of a cryogel.[7]

Solid State ^{29}Si NMR

The overall chemical environment of the silica surface can also be probed via ^{29}Si solid state NMR. A study describing a general characterization of several types of silica, including amorphous pyrogenic silica, was carried out by Leonardelli, et al. in which they were able to quantify the number of hydroxyl groups per square meter of surface area.[17,18] ^{29}Si NMR probes the actual chemical environment of the silicon atoms, and is not readily invalidated by certain limitations such as contamination, which might impede other characterization techniques such as IR spectroscopy. Additionally, there is some ambiguity as to when all water molecules adsorbed onto the silica surface are actually gone, due to the strong adsorption of water to silica surface, especially if any micropores are present. The adsorbed water molecules inside the micropores may not be driven off until 180°C.[17] Leonardelli, et al describe silica in several different chemical environments in their NMR study, three of which are:[17]

Q2: $Si(O_{0.5})_2(OH)_2$ the geminal (double) hydroxyl silanol groups

Q3: $Si(O_{0.5})_3OH$ the single hydroxyl silanol groups

Q4: $Si(O_{0.5})_4$ the siloxane groups which form the bulk of the material

According to the cited study the chemical shifts associated with each type of group are -91 ppm (Q^2), -100 ppm (Q^3), and -110 ppm (Q^4).[17]

Statement of Purpose

The purpose of this study is to determine if and how interactions between individual silica particles change as a result of the cryogelation process, or if they even exist at all. This characterization effort is focused mainly on the properties and changes in the presence and character of surface hydroxyl groups, both hydrogen bonded and non-hydrogen bonded. Overall morphology, such as pore size or the secondary, tertiary, etc. structure of cryogel samples can also affect its properties.[12] Since freezing and freeze drying are integral parts of the cryogelation process, this study seeks to characterize how these processes and other processing conditions affect morphology *as well as* surface chemistry. Is there any permanent or semi-permanent interaction between the primary silica nanoparticles? If so, how does this arise and how do processing parameters affect this interaction? Does the surface chemistry change in response to specific processing parameters, and what effect does this have on the final cryogel product? From a practical standpoint, successful completion of this study provides insight on how to concurrently influence the morphology, surface chemistry, and any particle-particle interactions between silica nanoparticles within a manufactured cryogel.

Experimental

Material Preparation

Silica cryogel samples were prepared in order to analyze their morphological and structural characteristics. Precursor slurries were prepared by manually mixing fumed silica (Cab-O-Sil HS5® **Cabot Corporation, Billerica, MA, USA)** with deionized and distilled (DDI) water. This was done by simply stirring the mixture in a beaker with a glass stir rod just until a visibly homogeneous mixture was obtained (~1 minute or slightly longer for higher amount of fumed silica). Unless otherwise specified, these slurries were frozen at -15 to -20°C for 48 hours. After freezing, the samples were placed directly into a lyophilizer (FreeZone Plus 2.5 Liter Cascade Benchtop Freeze Dry System from LABConco) to remove the excess water via sublimation, which typically took 24-36 hours. Each sample was also dried at 100 °C for 3-4 hours. Samples were prepared at 3, 4, 5, and 10 weight percent silica in DDI water. Each sample was modified in a unique way, adding, eliminating, or modifying steps to the above procedure. These modifications are detailed in Table 1 and also described more below. Samples **402 and 403** were sonicated in their initial slurry stage by placing the beaker containing the slurry in a bath sonicator (~30 kHz) for 5 and 25 minutes respectively. The pH of a 4 wt% slurry was measured via a Fisher Scientific pH probe to be 4.3. As explained later, this is consistent with other water-silica mixtures and it is assumed that all other slurries with the same proportion of silica have a pH of ~4.3. This is in contrast to sample **405**, whose slurry pH was adjusted manually to 10 (+/- 0.1) using a 1M NaOH solution. Sample **406** was covered with parafilm and stirred for 48 hours using a magnetic stir bar. The silica used to produce sample **407** was heated to 650°C prior to being incorporated into a slurry. Sample **502** was not frozen or freeze dried after the slurry was made, and was simply poured onto a watch glass and left to air dry.

Sample Numbers and Preparations			
Sample Number	**Processing Parameter**	**Sample Number**	**Processing Parameter**
301	Normal 3 wt% slurry	**406**	stirred 48 hours
301 A	Frozen 72 hours	**407**	Silica heated 650 C 12 hrs prior to slurry making, freezing and freeze drying
302	3 wt% frozen 11 days	**501**	normal 5 wt %
Bare	plain fumed silica	**502**	not frozen or freeze dried
401	Normal 4 wt% slurry	**502 crushed**	crushed up chunks before TGA
402	sonicated 5 mins (~30 kHz in a bath sonicator)	**503**	briefly frozen and freeze dried
403	sonicated 25 mins	**504**	frozen 48 hrs and air dried
404	pH 4.3, not adjusted	**1001**	10 wt%
405	Adjusted pH 10 with NaOH		

Table 1: Chart of sample numbers and unique processing condition if any. "Normal" indicates samples prepared using the standard procedure described.

Methods of Analysis

TGA

Thermogravimetric analysis was performed using a Q50 TGA manufactured by TA Instruments, New Castle, DE, USA. TGA analysis was conducted after drying the samples at 100°C overnight in order to drive off excess water. The analysis was conducted over a temperature range from room temperature to 800°C in N_2 with a heating rate of 10°C/min and a data sampling rate of 1 measurement/sec. Samples had a typical starting weight of ~15 mg, depending on the density of the powder. Weight loss was recorded as a percentage of the total

starting sample weight. As explained in the introduction, the three temperature regimes of interest were 100-200°C, 200-600°C and 600-800°C. Normally, several measurements would be made for each different sample to assess precision. However, multiple samples for each different cryogel could not be run due to time constraints, so a pooled standard deviation was established using multiple measurements of 3 different samples (**404**, **405**, and **504**). Four separate runs were conducted on each of the three aforementioned samples. From this data, a pooled variance, and eventually standard deviation, were calculated for three separate temperature ranges: 100-200°C, 200-600°C, and 600-800°C. The logic in this was that while the weight loss for each sample would be different, the variation in weight loss between measurements would be similar for each sample. Since all initial sample weights will be slightly different, the amount of evacuated compound, whether free water or hydroxyl groups, is expressed in terms of a percentage of the total sample weight. In this way, differences in weight loss can be used to compare the relative amount of water and hydroxyl groups present.

N_2 Adsorption

N_2 adsorption and subsequent analysis was performed on all samples in order to determine the surface areas and pore volumes. Nitrogen adsorption experiments were performed using ASAP 2010 and ASAP 2020 volumetric analyzers manufactured by Micromeritics, Inc. (Norcross, GA, USA). Adsorption isotherms were measured at -196°C over the interval of relative pressures (compared to atmosphere) from 10^{-6} to 0.995 using high purity nitrogen of 99.998 % from Praxair Distribution Company (Canton, OH, USA), which was used to measure the amount adsorbed as a function of the equilibrium pressure. Prior to each adsorption measurement, the sample was outgassed under vacuum in the port of the adsorption instrument for at least 2 h at 200 °C until the residual pressure dropped to 6 or less μm Hg. The specific

surface area (S_{BET}) was calculated according to the standard BET method .[19] The total pore volume was also evaluated via nitrogen adsorption at p/p_0 ~0.99 (p and p_0 denote the equilibrium and saturation pressure of nitrogen at -196 °C, respectively). The nitrogen desorption data were used to compute the pore size distribution using a self-consistent regularization procedure under non-negativity condition at a fixed regularization parameter $\alpha = 0.01$ with a complex pore model with slit-shaped and cylindrical pores, and voids between spherical nonporous particles packed in random aggregates.[20]

Bulk Density

The packing (bulk) density of the cryogel powders was measured by weighing a small amount of powder (~1-3 g) using a mg electronic balance, pouring it into a 10 mL graduated cylinder, and recording the volume of the sample after gently tapping the graduated cylinder for 60 seconds to ensure even settling. Packing density can indicate the relative density of secondary, tertiary, etc. particle aggregations. The denser the particle aggregates, the higher the packing density tends to be.

NMR

The surface chemistry of the silica cryogel powders was further characterized via solid state ^{29}Si NMR analysis. This was carried out using a 400 MHz - Bruker Avance FT-NMR spectrometer (Bruker Corporation, Billerica, MA, USA). Cross polarization and magic angle spinning (CP-MAS) were utilized to increase ^{29}Si signal intensity and to overcome signal broadening associated with solid state NMR. A 4 mm probe was used, the number of scans was 16,384 (a run time of about 14 hours), the sweep width was 30 kHz (380 ppm), the delay time between scans was 3.00 seconds and the CP contact time was 6 ms. The transmitter frequency (SFO1) for the Si nucleus was 79.4886563 MHz, while the transmitter frequency used for the ^{1}H

nucleus was 400.1314005 MHz. Deconvolution of the NMR data was carried out using NUTS by Acorn NMR Inc. A 20.00 Hz line broadening was assumed for exponential multiplication.

Results and Discussion

N_2 Adsorption and Bulk Density

The goal of these experiments was to determine if the aforementioned processing conditions affected any significant and persistent morphological (textural) changes on the fumed silica raw material. To this end, nitrogen adsorption was performed in order to characterize the surface area and pore volume of cryogel powders. Bulk density measurements were also performed for all samples and are mentioned here because they provide a useful comparison to the nitrogen adsorption data, and in turn these two characterization techniques yield useful information upon comparison to subsequent characterization techniques such as TGA. The first result of the nitrogen adsorption experiments can be seen below in Figure 4 which details the surface area of all samples.

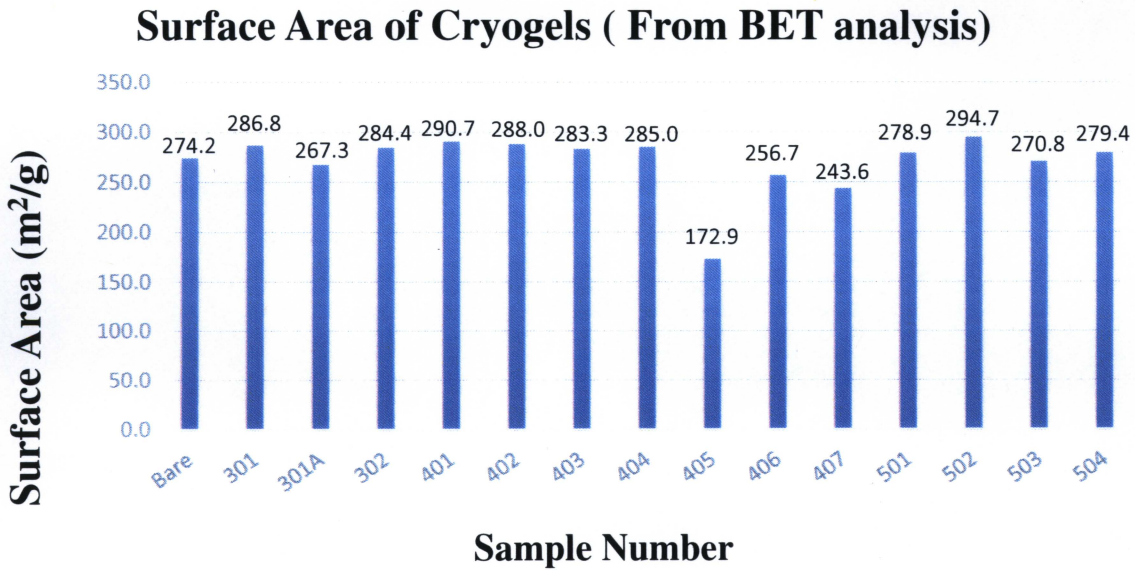

Figure 4. S_{BET} surface area of all silica samples as measured via N_2 adsorption.

Almost all of the tested samples maintained a surface area between 250 and 300 m^2/g. Only 2 samples have a surface area less than 250 m^2/g, samples 405 (base treated) and 407 (heat

treated), which constitutes a variation of >10% when compared to the surface area of the untreated bare silica of 274.2 m^2/g. One will recall that sample 407 was heated to 650°C for 12 hours. Formation of siloxane (Si-O-Si) bonds has been shown to occur as a result of the condensation of surface hydroxyl groups.[21] This is similar to what can occur in the initial stages of sintering. Sintering occurs when a material is heated sufficiently that atoms in the material lattice can diffuse freely from areas of high chemical potential, such as the outside surface of a material (where each atom does not have the ideal number of nearest neighbor atoms), to a region of lower chemical potential. In other words, the driving force for the sintering of a material is a reduction in surface area which reduces the surface free energy by lowering the amount of solid-vapor interfaces[13]. Studies using a combination of TG-DSC (thermogravimetric differential scanning calorimetry) and DRIFT (Diffuse Reflectance Infrared Fourier Transform spectroscopy) demonstrate that the condensation of hydrogen bonded hydroxyl groups present on the surface of the silica play a role in the initial sintering of the silica nanoparticles.[22,23] Specifically, the formation of new Si-O-Si bonds via condensation reactions between silanol groups contributes to densification. However, the low temperature of 650°C does not enable true sintering in this case, although the formation of siloxane bonds can occur. Different types of silica can exhibit sintering behavior at ~600°C, such as sol-gel derived silicas.[22] However, the small decrease in surface area for sample 407 is not due to the growth of the primary silica particles through sintering, but from overall effects of hydroxyl condensation. Hydroxyl groups contribute strongly to the hydrophilic character of the silica surface, and as they are driven off, the surface becomes more hydrophobic in nature.[5] The increase in hydrophobic character due to the 650°C pretreatment could have changed the aggregation of the nanoparticles, resulting in a lower measured surface area. One may wonder why the heating of the silica before cryogelation

processing still affects the surface area of the resulting powder after wetting, freezing, and freeze drying. Zhuravlev describes the re-hydroxylation process in a review paper, and is summarized in the figure below.[5] To summarize, re-hydroxylation of the silica surface occurs very easily

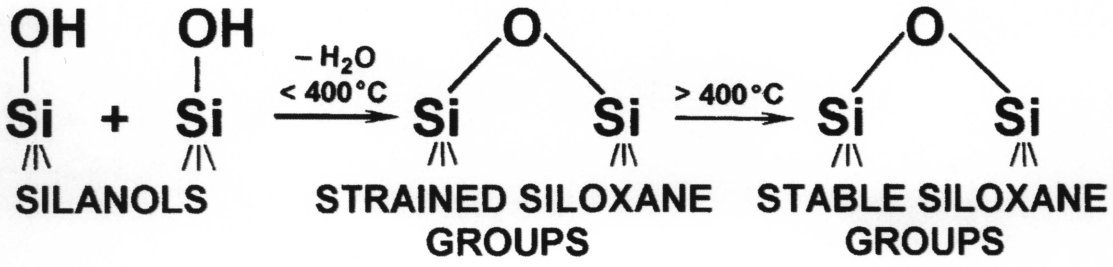

Figure 5. Diagram of the types of surface features on the silica surface that exist under different conditions.

when the material has been heated to *less* than 400°C. Below this temperature, enough hydroxyl groups exist on the silica surface to facilitate re-hydroxylation. Due to the hydrophobic nature of the Si-O-Si sections of the surface, a water molecule must first adsorb onto a nearby hydroxyl group before it can react with and break the siloxane bridge, forming new hydroxyl groups.[5] Being surrounded by so many hydroxyl groups, especially ones with adsorbed water molecules, actually helps to weaken the bond of the siloxane group, resulting in a relatively easy re-hydroxylation that can occur easily with the introduction of excess water. Above 400°C, the concentration of hydroxyl groups on the silica surface begins to decrease more rapidly than before, and the degree of hydroxylation θ_{OH} dips below 50% of the maximum.[5] At this point siloxane groups are no longer surrounded by so many hydroxyl groups and are converted into stable siloxane bridges which cannot be re-hydroxylated as easily or as quickly as their strained counterparts. Suffice it to say that sample 407 was heated well beyond 400°C and even exposure to excess water, freezing, and freeze drying were not enough to return the surface to a fully hydroxylated state. The resulting increase in hydrophobicity of the surface probably changed the packing behavior of the silica particles, resulting in a lower measured surface area.

The base treated sample 405 exhibited an even lower S_{BET} surface area than the heat treated sample 407. Reduction in surface area in this case is most likely caused by the increase in size of the primary silica nanoparticles. According to Iler, the solubility of silica in water increases drastically at high pH (> 10).[1] This effect is more pronounced the smaller the silica particles. Essentially, the smallest silica particles dissolve in the high pH water and re-deposit in the crevices between larger particles. This results in the overall reduction of surface area and an increase in average particle size. Table 2 shows the calculated particle size for each sample based on the surface area while assuming a spherical particle shape and no closed porosity. The high pH conditions in the silica slurry of sample 405 (pH of 10) resulted in a drastic increase in particle size over samples 401 and 404, which had a pH of only 4.3 in the slurry stage, subjected to identical conditions making these two materials replicates of one another.

Sample	Surface Area (m^2/g)	Calculated Particle Diameter (nm)
401	290.7	9.38
404	285.0	9.56
405	172.9	15.77

Table 2. Calculated particle size of selected samples based on their measured surface area (via nitrogen adsorption) and assuming a spherical particle shape. The equation for particle size is: $D = \frac{6000}{\rho\,(SSA)}$ where D is the particle diameter, ρ is the density of amorphous silica (2.2 g/cm^3), and SSA is the specific surface area of the material in m^2/g.

Bulk density measurements also pointed to a change in sample morphology as a result of the processing used in this study. Below, Figure 6 shows results of the bulk density measurements for all samples. As expected, the bare silica exhibited the lowest bulk density of all samples. This material easily formed a dust and had a very fine texture and appearance. After processing, samples became noticeably compacted and did not form a dust nearly as easily as the

bare silica. An increase in bulk density can be attributed to rearrangement of the primary silica particles into larger secondary, tertiary, etc. clusters. Nanoparticulate silica has been shown to form larger, more compacted clusters after similar processing, certainly more so than when the bare silica is formed from the flame.[8] One will notice that sample 405, whose particle size has increased from the high pH treatment during the suspension phase, does not differ greatly from other cryogels in terms of bulk density. Though the particle size of the silica has increased, the overall packing behavior of the nanoparticulate silica does not seem to have been greatly affected in this case.

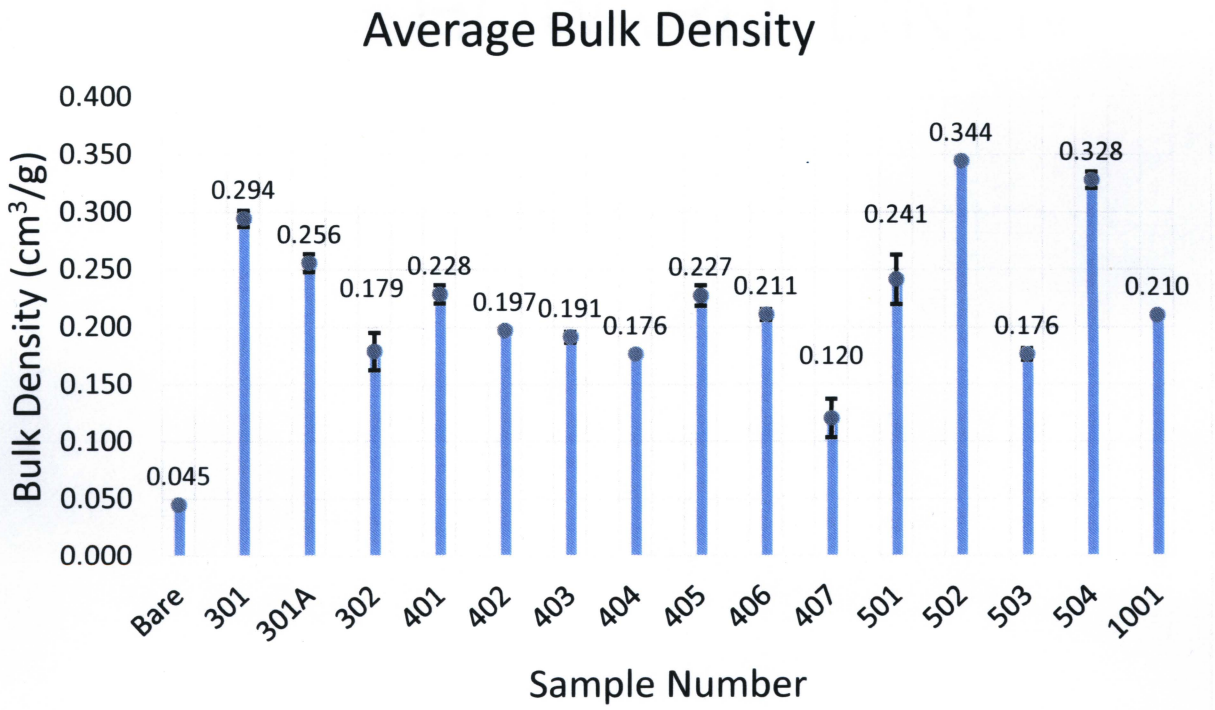

Figure 6. Bulk density measurements for all dry sample powders. Error bars indicate one standard deviation calculated from 3 replicate measurements of bulk density.

Although a high variability exists in the bulk densities of cryogel samples, the main point of bulk density measurements is to point out the differences between cryogel samples and unprocessed or partially processed silica. One or more of the processing techniques used results

in a significant change in the bulk density of the starting powder, which can also be seen from the overall appearance of the sample. Figure 7 shows a cryogel sample which has been both frozen and freeze dried. The freeze drying process appears to be one of the reasons for the course powdery consistency of lyophilized samples. Although not *exactly* the same, freeze dried samples all appear to have a similar texture. In contrast, sample 502, which was not frozen or freeze dried but only air dried after suspension, formed large semitransparent chunks when dried, which can be seen in Figure 8. The distinct appearance of sample 502 seems to somewhat reinforce the differences in bulk density seen in Figure 6.

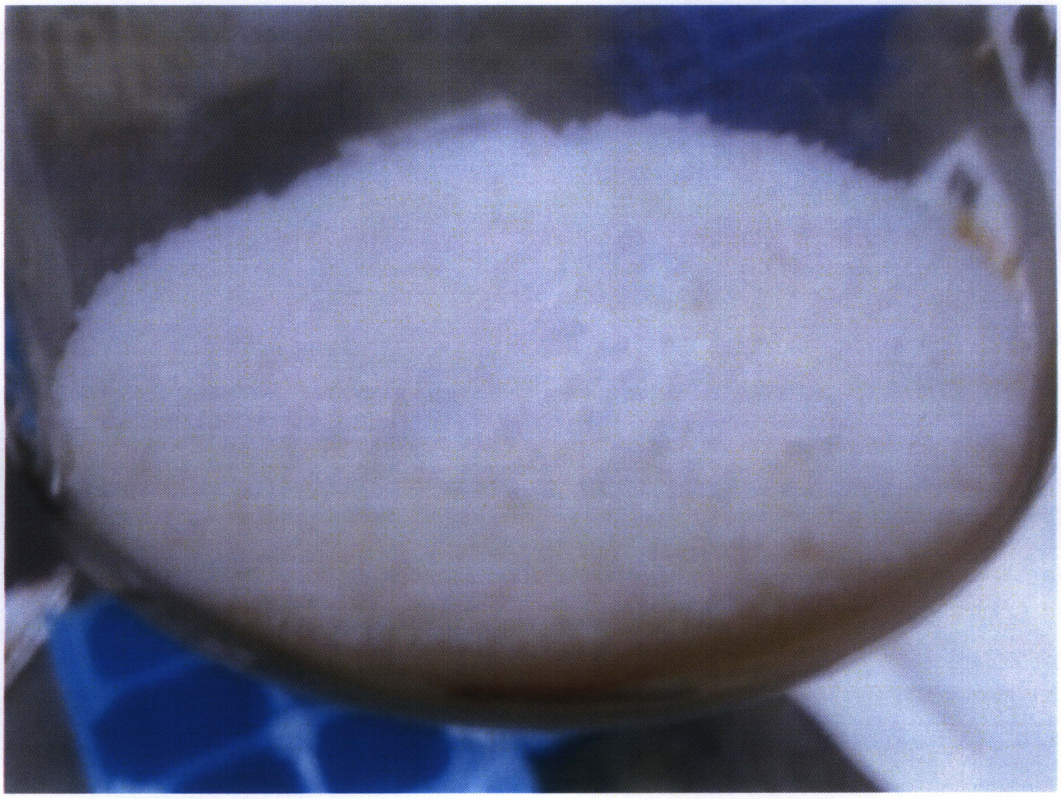

Figure 7. Frozen and freeze dried cryogel powder in its glass lyophilization container. Notice the slightly course texture.

At the very least, a difference in particle aggregation arises because of the freeze drying process. A simple comparison of Figures 7 and 8 clearly indicates a difference in the outward appearance of the macroscopic aggregation of a non-freeze dried and freeze dried sample respectively. Bulk density measurements also show a difference between samples that were freeze dried (e.g., sample 503) and samples that were not freeze dried, but merely frozen and air dried (sample 504) or even just mixed with water and air dried (502). The two samples that were not freeze dried, samples 502 and 504, have a higher bulk density than the freeze dried samples. The freeze dried samples seem to exhibit a high degree of variation, even between comparable samples. For example, samples 401 and 404 were both made by freezing and freeze drying a 4 weight % silica-water slurry. However, as seen in Figure 6, the variation in bulk density between 401 and 404 is 0.052 g/cm^3 (~29%) even though these samples were prepared using the same procedure.

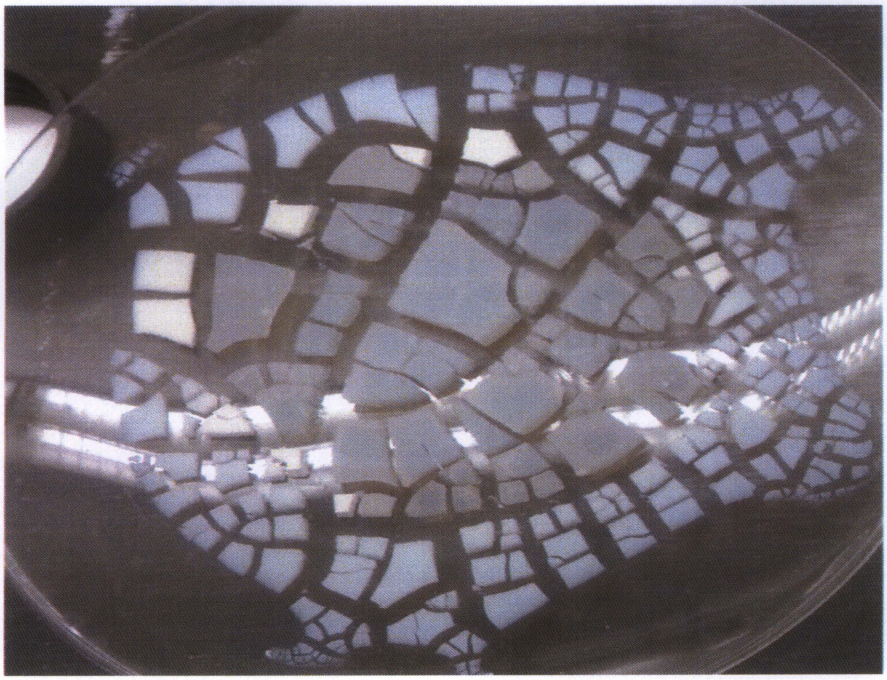

Figure 8. Sample 502, nanoparticulate silica simply suspended in water and poured onto a watch glass and left to air dry. This differs greatly from the freeze dried sample shown in Fig. 9.

In Figure 8, the drying mechanism of the air dried sample 502 can be inferred based on appearance alone. As the excess water evaporated, the silica-water slurry becomes thicker and more viscous until the thickened slurry starts to pull apart. The large amount of shrinkage due to drying causes the large cracks and crevices apparent in the sample pictured in Figure 8. At the same time, the fact that the slurry was not frozen allowed the silica particles to have at least some mobility within the slurry during the drying process. Therefore silica particles and their secondary, tertiary, etc. formations were all allowed to coalesce to form relatively dense structures thanks to the slow drying process. This resulted in the relatively high bulk density for the air dried samples. The agglomerates and aggregates of silica inside freeze dried samples do not have the luxury of mobility during the drying phase, and are locked in place until released by the sublimation of the surrounding ice. Figure 9 shows a photograph of a cryogel sample part

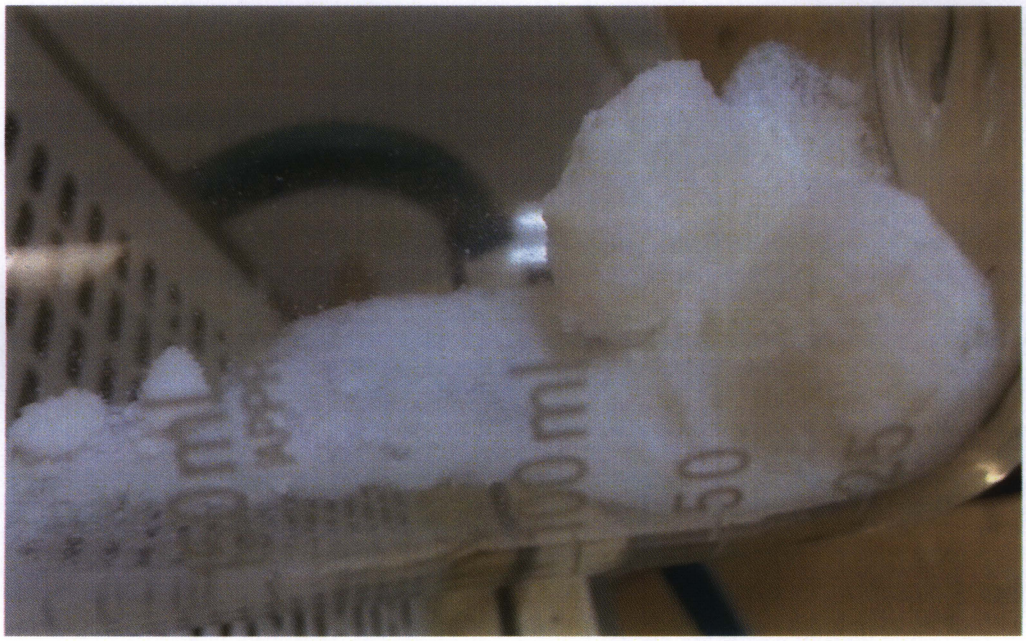

Figure 9. A cryogel sample in the midst of freeze drying. The slow release of the silica from the ice as a result of sublimation contributes to the coarse powdery texture of the cryogel.

way through the freeze drying process, which shows how aggregates flake off as they are freed from the ice. Although the primary silica particles were probably squeezed together by the freezing process to be locally dense, the complex and somewhat random arrangement of the particles in the slurry upon freezing seems to create a less dense sample, with more diffuse collections of aggregates than the air dried samples.

So far the comparisons made between samples using surface area, bulk density, and overall appearance point to significant differences between the bare silica, manufactured cryogels, and samples (502) and 504, which were not freeze dried. One last interesting morphological phenomenon observed for the cryogel powders was that the sample retains the same outward appearance after re-immersion in water and air drying. Figure 10 shows a previously frozen and freeze dried powder that was re-immersed in water (at a concentration of ~4-5 wt%) and allowed to air dry. Surprisingly, the sample does not cake up like sample 502

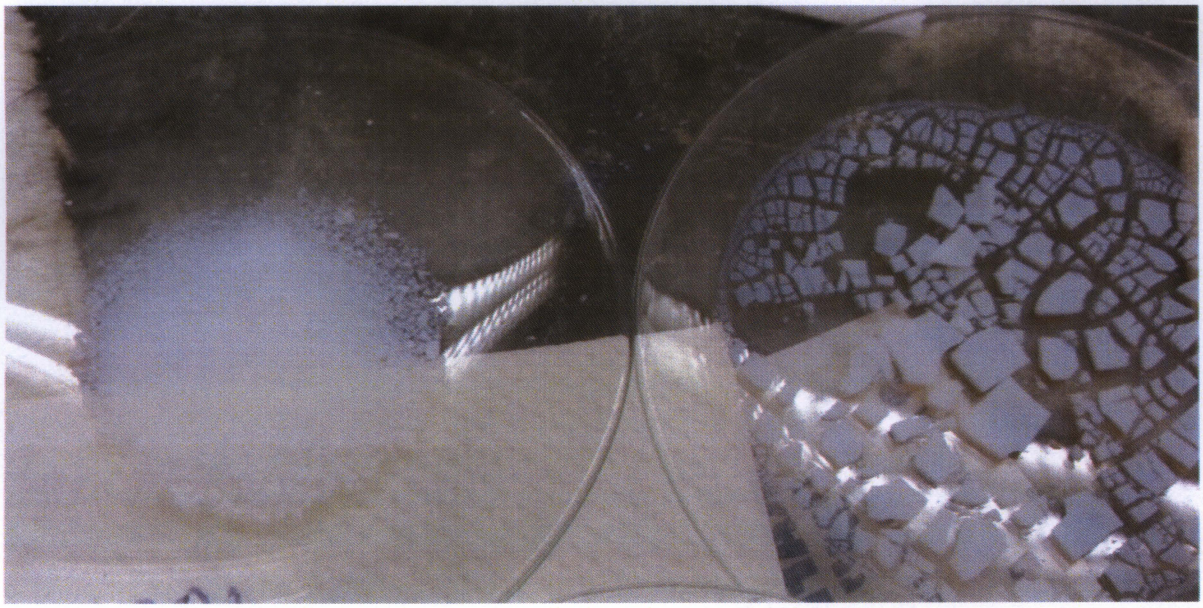

Figure 10. On the left is a previously frozen and freeze dried cryogel powder that was re-immersed in water and allowed to air dry. On the right is a sample not frozen or freeze dried, but simply air dried from the initial silica-water slurry.

(pictured on the right in the same photo) but instead remains a coarse-looking powder. While it cannot be specified if the morphology is *exactly* the same as before immersion and drying, its appearance and texture are at least very similar to its previous state, and very different from samples that were originally air dried. This would seem to indicate that the morphology or possible interaction between silica particles is not perturbed by simple immersion and mixing action. Additional testing would be required to ascertain how much physical agitation or how prolonged such agitation would need to be to change the post-processing morphology of the cryogel.

Additional information from nitrogen adsorption regarding pore size and pore size distribution is detailed below. Conventions for describing pore sizes in silica cryogels have been described in previous literature.[8] Different classes of pores are described as follows: *nanopores* have a radius of $R < 1$ nm, mesopores have radius of $1 < R < 25$ nm, and macropores have a radius of $R > 25$ nm. The only size limit for classifying macropores is the capability of N_2 adsorption technique to detect them. Nitrogen cannot effectively fill large pores, and so in this experiment, only pore sizes up to a radius ~40-50 nm can be accurately characterized by N_2 adsorption. We thus define macropores as pores with radius $25 < r < 40$ nm. The amount of pore volume in each size regime is given in terms of volume per unit weight of sample (cm^3/g). The remainder of pores and other vacant space (with $r > 40$ nm) cannot be characterized via nitrogen adsorption, but the volume of the remaining space can be calculated using equation 6, where V_{em} is the volume of empty space and/or pores with $r > 40$ nm, ρ_b is the bulk density of the

$$V_{em} = \left(\frac{1}{\rho_b} - \frac{1}{\rho_0}\right) \quad (6)$$

powder, and ρ_0 is the density of amorphous silica ($2.2 g/cm^3$).[8] $1/\rho_0$ simply gives 0.454 cm^3/g in this case. To summarize, we can now separate the voids in our silica cryogel material into four categories: nanopores, mesopores, macropores, and empty space not measurable by nitrogen adsorption. The relative volume of the pores in each category, compared with surface area measurements and bulk density, can yield information about how different processing techniques influence aggregation and agglomeration of the primary silica nanoparticles.

A higher bulk density in cryogel powders corresponds to more closely packed particles, agglomerates, and aggregates and by extension a larger amount of pores of a measureable size ($r < 40$ nm). A graph of the total pore volume for each sample can be seen in Figure 11, and this indeed seems to mirror the variation of values in the bulk density measurements, seen in Figure 6. A plot of pore volume vs. bulk density, Figure 12, illustrates that pore volume increases with bulk density. The total pore volume is quite low for the bare silica (as expected), and all cryogel samplesexhibit an amount of measurable (by N_2 adsorption) pore volume greater than the bare sample. The size distribution of the pores in each sample seem to reflect similar information.

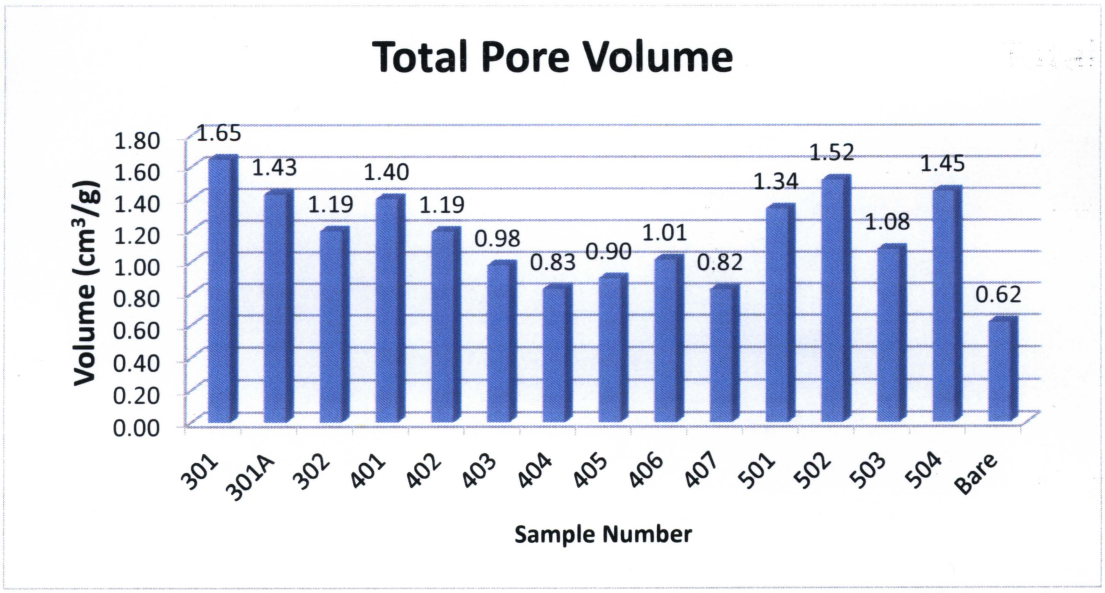

Figure 11. Total pore volume of samples summed from pore volume distribution data.

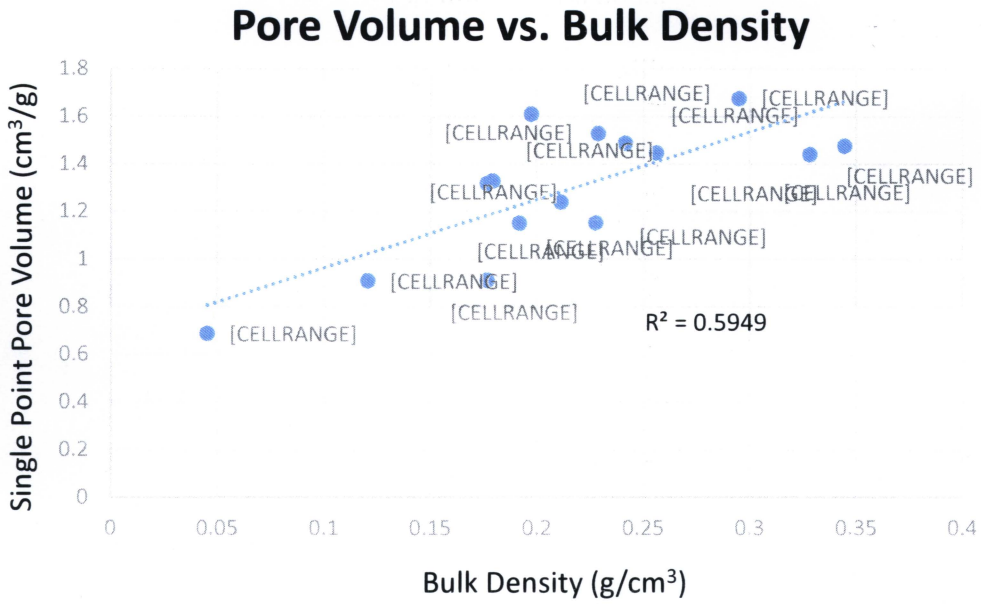

Figure 12. Pore volume vs. bulk density showing overall trend in data.

Figures 13 and 14 show the pore size distribution from a diameter of 1 nm to ~80 nm (10-800 Å). In Figure 13, notice the overall pore volume of the bare silica remains quite low over the measured size range in comparison to the cryogel samples. The 3 wt% samples pictured in Figure 13 exhibit significant differences between one another. In this case, samples 301, 301A, and 302 signify an increase in freezing time during sample processing. As a reminder, sample 301 was frozen for 24 hours, 301A for 72 hours, and 302 for 11 days. All 3 wt% samples and most other cryogel samples appear to have relatively few pores with a width below 100 Å. Above the size of 100 Å, pore volume steadily increases and then enters a regime in which the pore volume fluctuates considerably while remaining higher than the <100 Å regime. Figure 13 indicates a decrease in pore volume with increasing freezing time. The pore

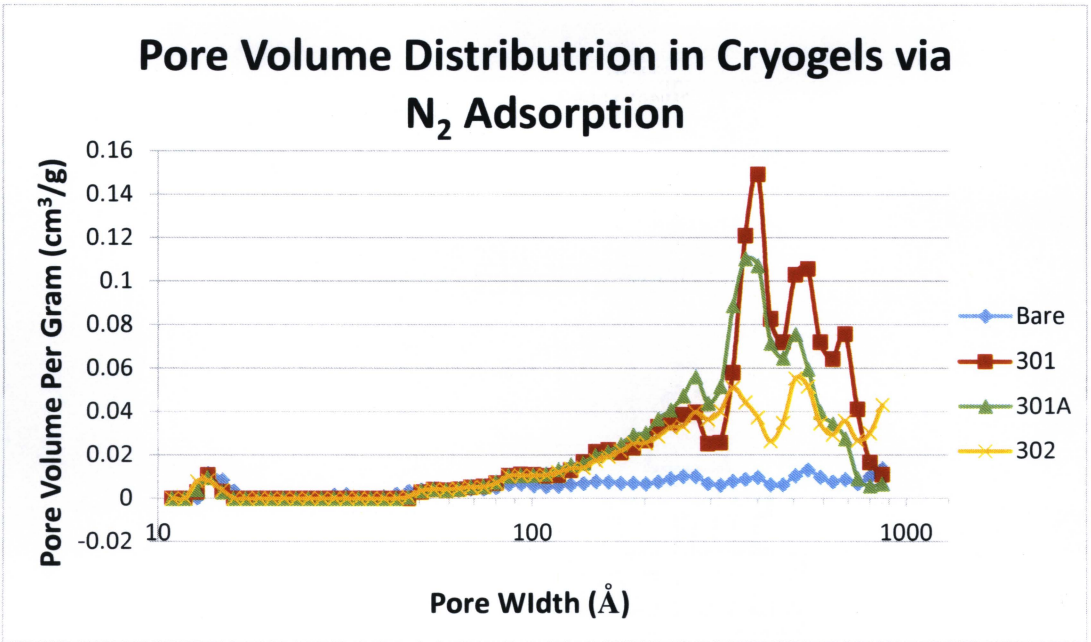

Figure 13. Pore volume distribution of bare silica and all 3 wt% samples showing a general decrease in pore size with freezing time. This is especially true for pore widths of ~200-600 Å.

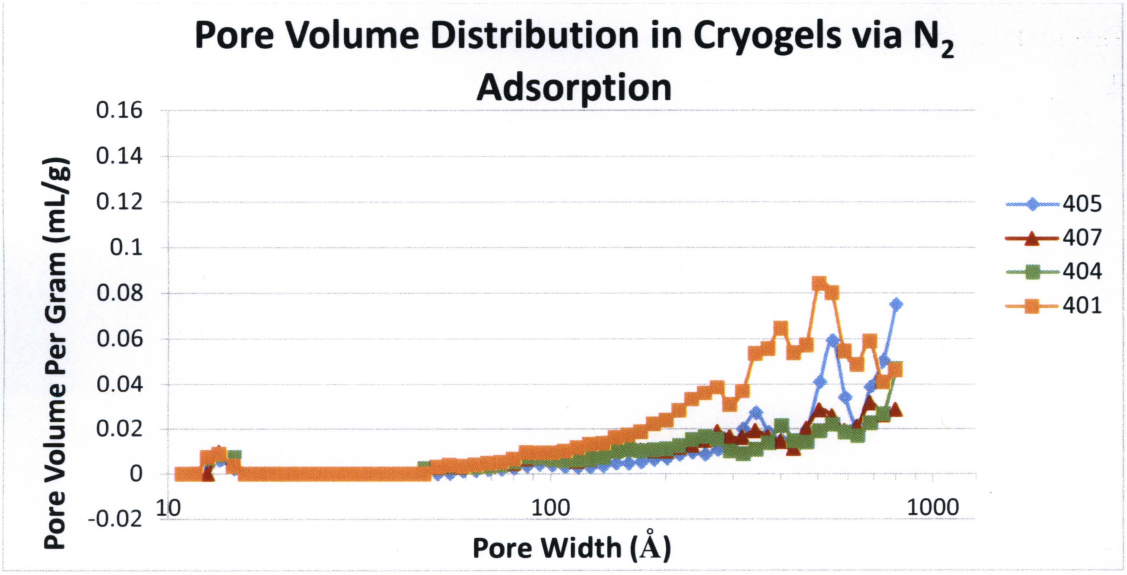

Figure 14. Comparison of various 4 wt% samples, including 401 and 404 which had identical processing parameters.

volume distribution shown in Figure 13 mirrors this relationship among most pore sizes, except for a small area around 300 Å. The bulk density measurements from Figure 6 also reflect this trend. All cryogel samples in Figure 13 also exhibit a solid difference from the bare silica. The

apparent correlation between freezing time and pore volume can be called into question by the variability in the pore volume distribution between identically processed samples (401 and 404).

The pore distribution and total pore volume of identically processed samples varies fairly widely. Sample 401 and sample 404 (both simple 4wt% cryogels) were processed in the same fashion, and yet their pore distributions differ significantly, in total pore volume as well as in the variability of pore volume with increasing pore size. Figure 14 shows the difference in pore size distribution between these samples. This discrepancy might be related to the consistency of the cryogel powders post processing. Cryogel samples were not perfectly uniform and contained macroscopic aggregates of different sizes. Large chunks of cryogel materials may have contained pores not able to be accessed by N_2 adsorption. The chaotic nature of the freezing and freeze drying process may also just result in inconsistent samples. In any case, the large variance in pore volume between 401 and 404 should be kept in mind when drawing conclusions about processing parameters.

Figure 15 shows the pore distribution of the 5 wt% samples, including the non-freeze dried samples. Note that the data for sample 502 (not frozen or freeze dried) is only valid up to a pore width of ~400 Å. One can clearly see the difference in the pore volume distribution between different samples, such as 501 (5 wt%), which has more large pores, and sample 504 (base treated), which has more small pores. Sample 501 (normal 5 wt%), 504 (frozen and air dried), and 502 (not frozen or freeze dried) all have a larger pore volume than sample 503 (briefly frozen and freeze dried). This can be seen in Figure 11 as well as Figure 15. This holds true over the whole range of pore sizes in Figure 15 except for the very largest.

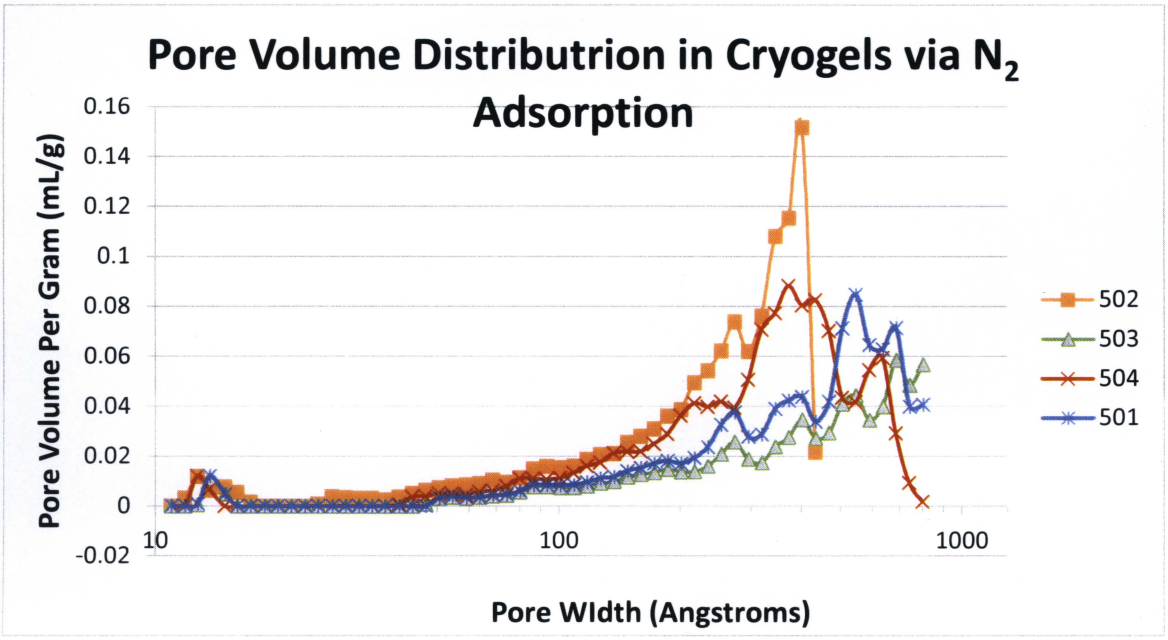

Figure 15. Compares 5 wt% samples not frozen, not freeze dried, or both along with a normal 4 wt% sample. Note the inconsistency in 502 where data was cut short.

A more specific breakdown of the pore volume distribution can be seen in Figures 16 and 17, which show the pore volume of mesopores and macropores, respectively, as a percentage of total measured pore volume, for all samples. Comparing the relative amounts of each type of pore formed may yield more information, since total pore volume seems to vary widely because of the nature of the freezing and freeze drying process. Of the categories of pores discussed here (nano-, meso-, and macropores) mesopores account for well over 50% of the pore volume present in all samples; even for the bare silica. Since the percentage of nanopores in each sample is very low, a larger proportion of mesopores results in a smaller proportion of macropores and vice versa. Since the percentage of nanopores in each sample is very low, a graphical representation of their relative proportions would have little value. The amount of nanopores ($r <$ 1nm) present is less than 1.5% by volume in all cases. Although identically processed samples

401 and 404, had very different total pore volumes, the volume percentage of mesopores present in each sample, 80.2% and 82.4%, are nearly identical.

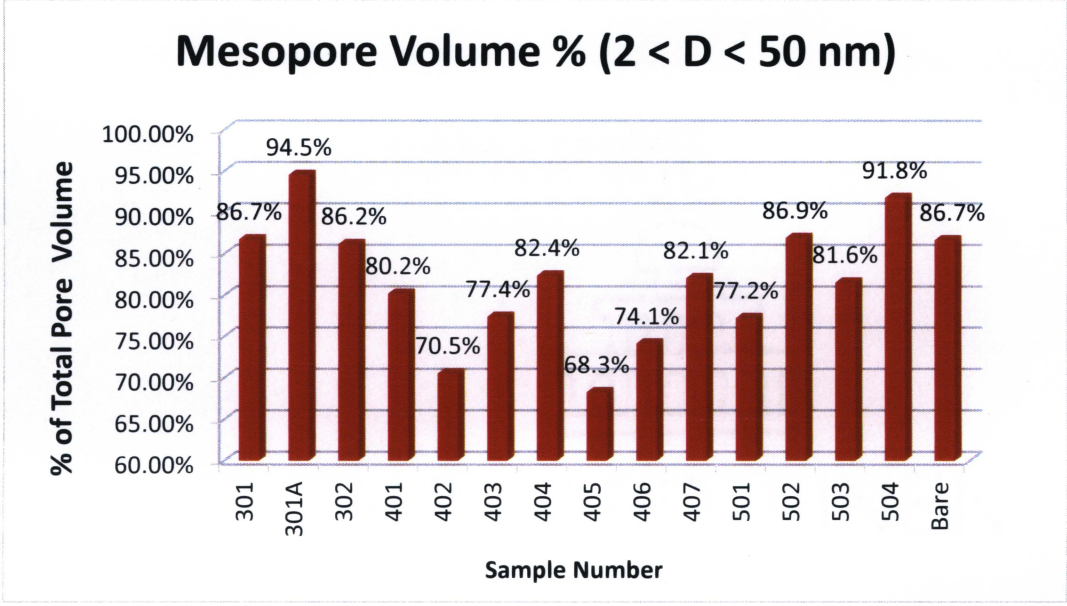

Figure 16. Mesopore volume of each sample as a percentage of total pore volume. Y axis adjusted for ease of comparison.

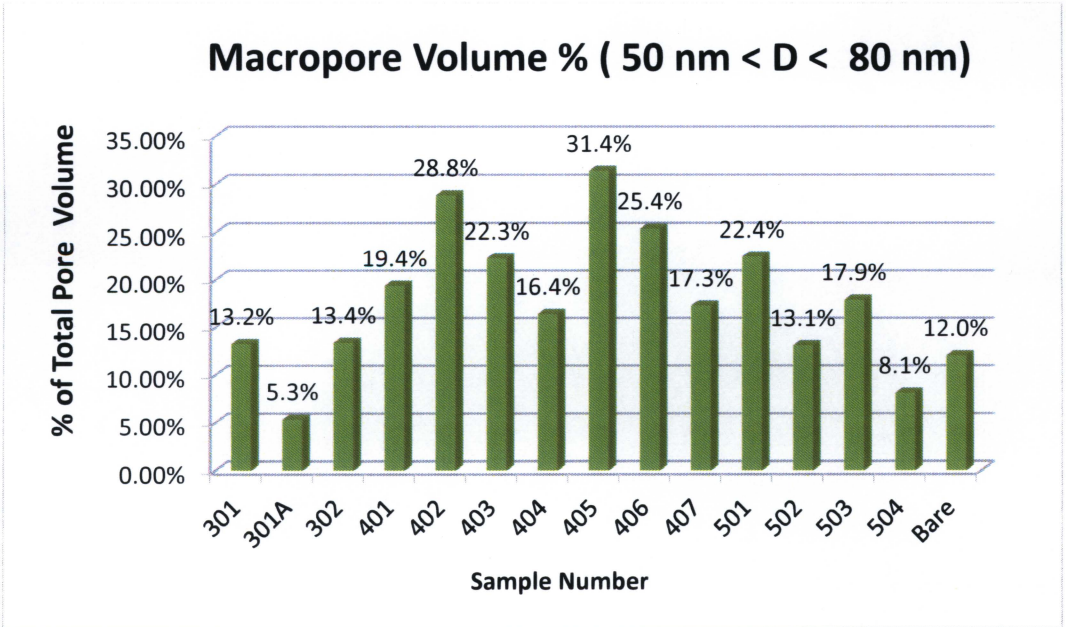

Figure 17. Macropore volume as a percentage of total pore volume in each sample

Samples 404 (un-altered slurry pH of 4.3) and 405 (base treated to pH 10), which were shown to have a very similar total pore volume in Figure 11, have dissimilar amounts of mesopores, with sample 405 having a substantially lower percentage of mesopores, and thus a higher percentage of macropores, than sample 404. This is likely due to the enlargement of the primary silica nanoparticles in the pH adjusted sample 405 (pH 10). Larger primary particle size would make it less likely that very small pores can form. Sample 407, the heated 4 wt% sample, has a very similar percentage of mesopores in relation to sample 401 and 404. Sample 407 was prepared as a regular 4 wt% sample, just like 401 and 404, but only after the silica used to manufacture it was heated to 650°C for 12 hours. Heating to such a temperature can change the surface chemistry of the silica, as discussed in previous sections, but this does not seem to drastically affect the type and proportion of pores that are able to form during processing.

One last bit of information gleaned from N_2 adsorption data was the volume of empty space (V_{em}), calculated using Equation 6. Figure 18 shows V_{em} for each sample which reaffirms

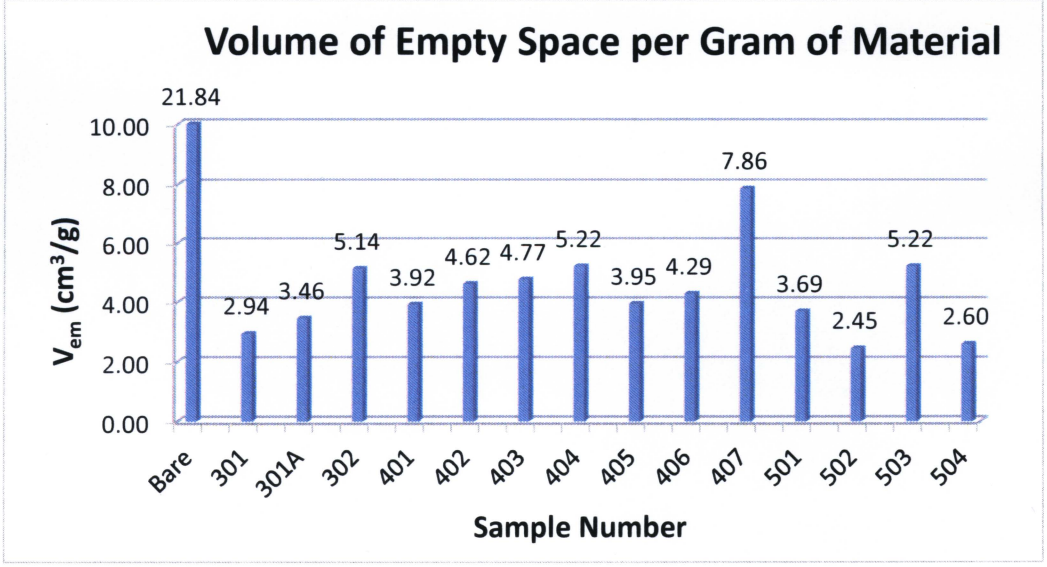

Figure 18. Volume of empty space (pore radius r > 40 nm) in cryogel samples in volume per gram of material.

the fact that a clear difference exists between the bare silica and the cryogel samples. The amount of space not considered to be pores (r > 40nm) was greatest in the bare silica, at 21.84 cm^3/g, with sample 407 (heat treated prior to cryogelation) second at 7.86 cm^3/g. The high amount of empty space in sample 407, and its correspondingly low overall pore volume, seems to indicate that heating of the silica prior to cryogelation significantly impacts the packing behavior of the final product. These differences can be compared more easily in Table 3, which

Data Summary for Bulk Density and N_2 Adsorption Analysis

		Average Bulk Density (g/cm^3)	Single Point Pore Volume (cm^3/g)	Mesopore Volume % (cm^3/g)	Macropore Volume % (cm^3/g)	V_{em} (cm^3/g)
larger sample	**Bare**	0.045	0.69	86.73%	13.23%	21.84
3 wt % frozen 48 hrs	**301**	0.294	1.68	94.53%	5.32%	2.94
3 wt% frozen 72 hours	**301A**	0.256	1.45	86.18%	13.36%	3.46
3 wt% frozen 11 days	**302**	0.179	1.33	80.21%	19.36%	5.14
Normal 4 wt%	**401**	0.228	1.53	70.54%	28.81%	3.92
sonicated 5 mins	**402**	0.197	1.61	77.40%	22.26%	4.62
sonicated 25 mins	**403**	0.191	1.15	82.40%	16.39%	4.77
pH 4.3	**404**	0.176	0.91	68.27%	31.37%	5.22
pH 10	**405**	0.227	1.15	74.15%	25.36%	3.95
stirred 48 hours	**406**	0.211	1.24	82.10%	17.27%	4.29
heated 650 C 12 hrs	**407**	0.120	0.91	77.24%	22.44%	7.86
normal 5 wt %	**501**	0.241	1.49	86.92%	13.08%	3.69
crushed up chunks before TGA	**502 crushed**	0.344	1.48	81.56%	17.89%	2.45
briefly frozen and freeze dried	**503**	0.176	1.32	91.77%	8.08%	5.22
frozen 48 hrs and air dried	**504**	0.328	1.44	86.65%	12.00%	2.60
10 wt%	**1001**	0.210				

Table 3. Summary of data for bulk density, pore volume, and V_{em} for all samples. Nanopore volumes for each sample were omitted as they were very small compared to other pore volumes (<1 volume %).

contains all data discussed thus far for each sample. The total pore volume of sample 407 is very similar to that of sample 404, as seen in graph 10. Yet sample 407 has a lower bulk density and a higher amount of empty space (V_{em}). The only factor separating sample 407 from samples 401 and 404 was the fact that its silica was heated to 650°C before cryogelaton. This factor seems to have been the cause of lower bulk density and high V_{em} in sample 407. As described in previous sections, the hydroxyl content of the silica surface in sample 407 is likely to have been dehydroxylated to a point where 50% or more of its surface hydroxyl groups are gone. Furthermore, any re-hydroxylation will occur quite slowly at room temperature, and certainly no faster at -15°C.[5] It seems that the loss of hydroxyl groups affected the way the silica nanoparticles form agglomerates and aggregates during the cryogelation process. The result is a lower bulk density and higher V_{em} (7.86 cm^3/g) than other cryogel samples. The next highest V_{em} values were samples 404 (normal 4 wt%) and 503 (briefly frozen and freeze dried), both at 5.22 cm^3/g. This constitutes an increase of 50.5% in V_{em} from samples 404 and 503 to sample 407. In addition, sample 407 had a relatively low pore volume (0.91 cm^3/g), though it was comparable to that of several other samples (e.g 404 also at 0.91 cm^3/g). The important conclusions about the processing conditions of sample 407 and other samples are itemized below for convenience and clarity, while data is present in Table 3.

Freezing Time - Samples 301, 301A, and 302. Samples were frozen 48 hours, 72 hours, and 11 days respectively. This data is shown below in Figure 19. Also, as seen in Figures 6 and 11 (or Table 3), bulk density and pore volume seem to decrease with increasing freezing time.

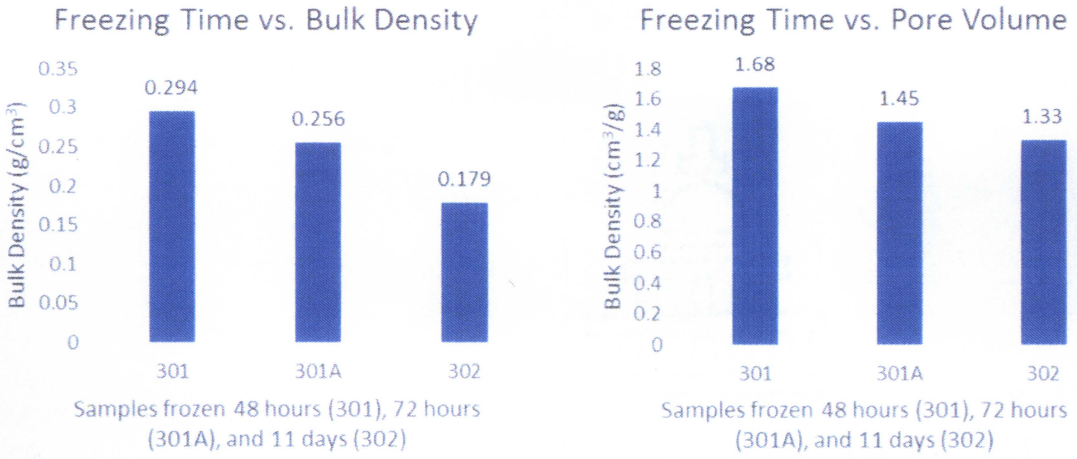

Figure 19. Graphs detailing the relationship between freezing time, bulk density, and pore volume.

Sonication - Samples 402 and 403 were sonicated for 5 minutes and 25 minutes respectively in a bath sonicator while in slurry form, prior to cryogelation. The original goal was to see if samples that were well dispersed would behave differently than samples that were only hand mixed. This is of course assuming sonication in this manner would be any better than mixing by hand, especially considering the hydrophilic surface of fumed silica, which favors dispersal in water. See Figure 20.

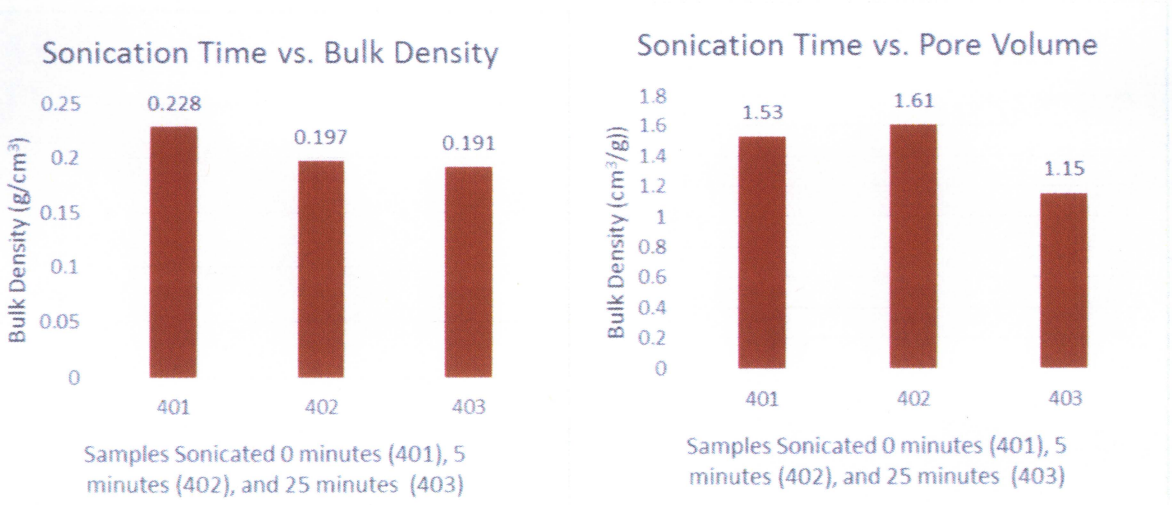

Figure 20. Graphs detailing the relationship between sonication time, bulk density, and pore volume.

Bulk density for these samples was very similar and the pore volume for sample 402 was slightly higher.

pH Adjustment - Sample 404 and 405 were tested for pH at the slurry stage. Sample 404 was left at its unadjusted pH of 4.3 before cryogelation, and sample 405 was adjusted with NaOH until its slurry reached a pH of 10. The total pore volume for each sample is similar while 405 had a higher bulk density than sample 404. Note again that sample 405 had a significantly smaller surface area, and larger primary particle size, due to high pH treatment as discussed previously. This can be seen below in Figure 21. The intricacies of this phenomenon are discussed more in depth later in the report.

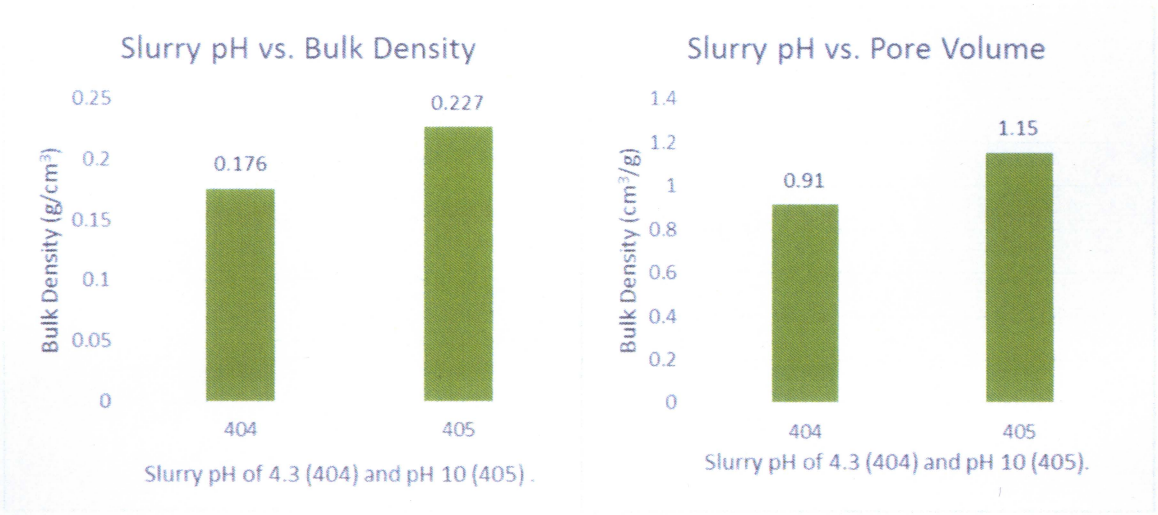

Figure 21. Graphs detailing the relationship between slurry pH during cryogel production, bulk density, and pore volume.

Heat Treatment - As mentioned above, sample 407, whose silica was heated prior to cryogelation, exhibited a low bulk density and high V_{em} in relation to other cryogel samples. The pore volume is also low for this sample, but deviates much less from the other cryogel samples in this regard. This can be seen in Figure 22. The loss of surface hydroxyl groups most likely

affected the packing behavior of the silica in question by increasing the hydrophobicity of the surface.

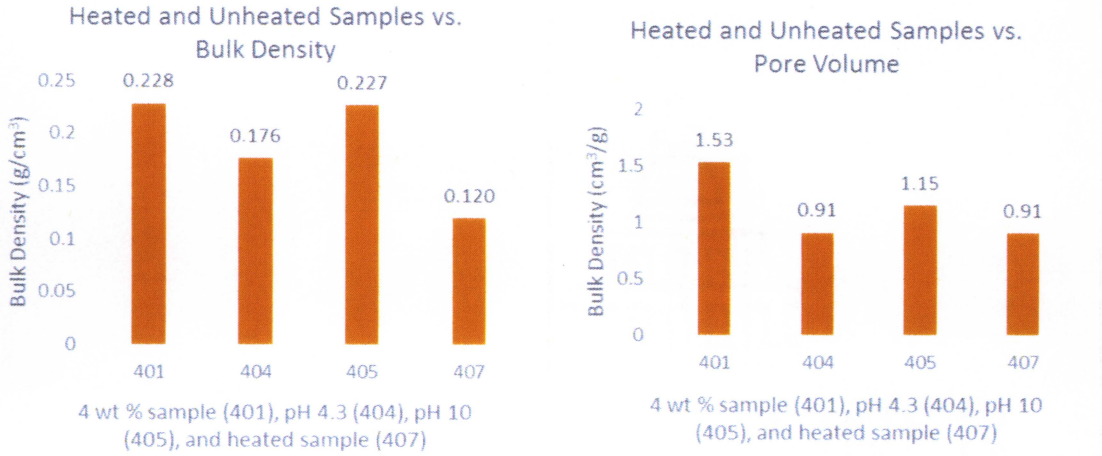

Figure 22. Graphs comparing various samples whose silica was NOT heat treated prior to cryogelation and a sample whose silica WAS heat treated prior to cryogelation (407).

Frozen vs. Not Frozen – Two samples that can be compared when considering the parameter are sample 502, which was not frozen or freeze dried, and sample 504, which was frozen for the normal 48 hours and air dried (not freeze dried). These samples are quite similar in both bulk density, which was high compared to other cryogels, as well as pore volume. Freezing alone does not seem to appreciably affect these properties. See Figure 23 below.

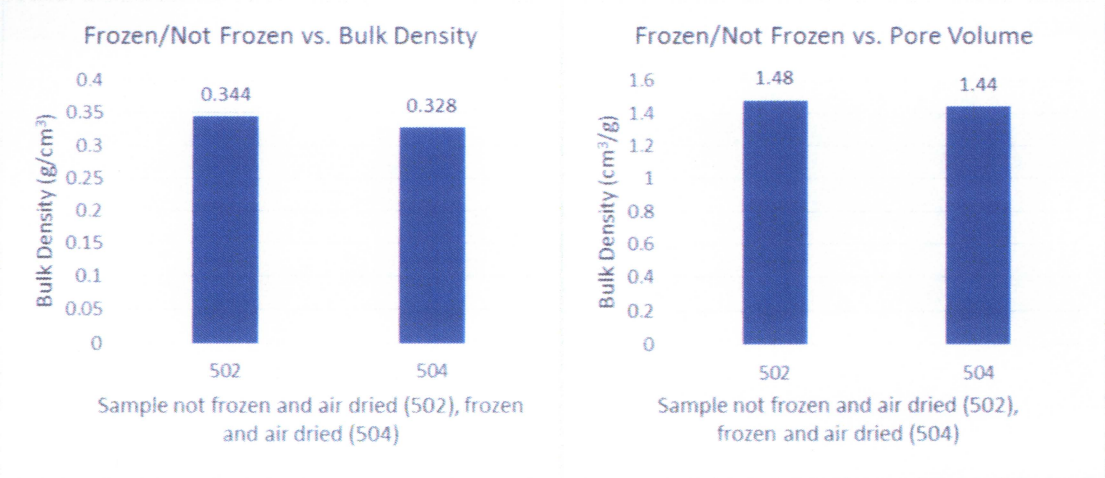

Figure 23. Graphs detailing the relationship between freezing (504), or not freezing (just dispersion in water 502), to bulk density and pore volume. Both samples were air dried.

Freeze Drying vs. Air Drying – One will remember from Figure 8 that air dried samples formed large semi-transparent chunks upon drying from the starting slurry. Both of the air dried samples, 502 and 504, exhibited the highest bulk density among all samples, being almost 3x as dense as sample 407, which had the lowest bulk density among cryogel samples. 502 and 504 also exhibited a somewhat high pore volume among the cryogel samples. Freeze dried and air dried samples appear very different macroscopically, and although air dried samples seem to have a higher overall bulk density, their pore volume is very similar to freeze dried samples.

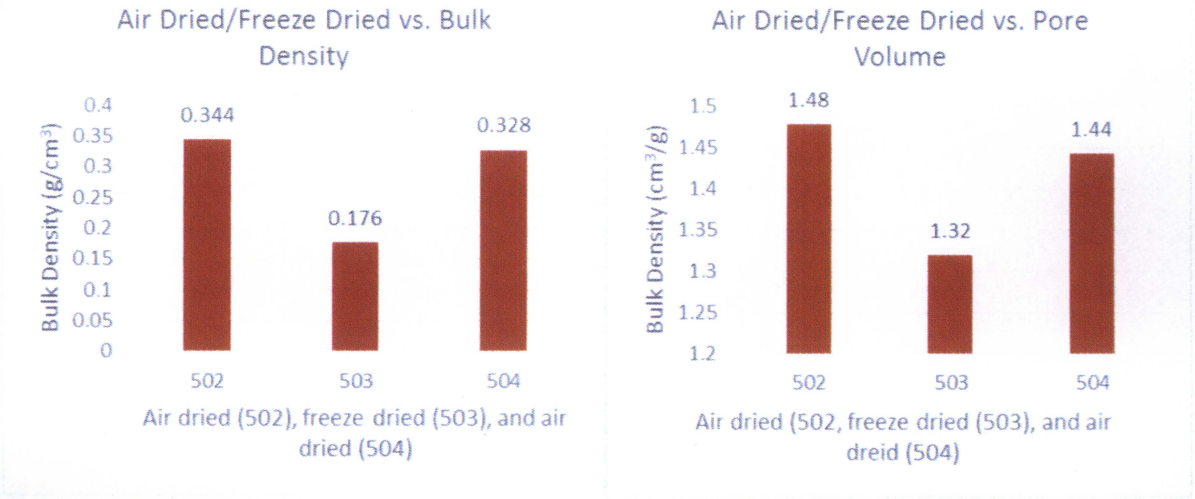

Figure 24. Graphs comparing air dried samples (502 and 504) to a freeze dried sample (503). Sample 502 was not frozen but was air dried, sample 503 was frozen only briefly and freeze dried, and sample 504 was frozen but air dried. Therefore, samples 502 and 504 may be compared with sample 503, though not directly with each other. Notice the adjusted scaling on the Bulk Denisty vs. Pore Volume graph.

Solids Loading – Sample 301, 401, 501, and 1001 differ from each other only because of the weight % of silica used to manufacture their initial slurry (3, 4, 5, and 10% respectively). Sample 301 has the highest bulk density and pore volume, followed by samples 401 and 501, which are very similar (Figure 25). Lastly, sample 1001 has the lowest bulk density and pore volume out of the four samples. It seems that higher solids loading in the initial slurry results in a lower overall bulk density and pore volume. Note that the pore volume of sample 1001 was not measured.

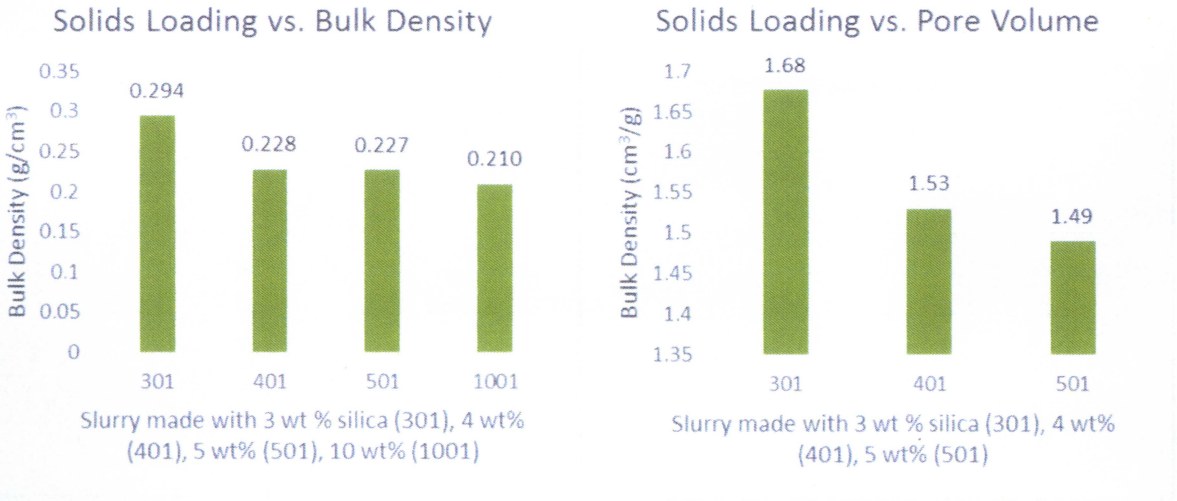

Figure 25. Graph comparing the solids loading of the slurry made during cryogel manufacture with bulk density and pore volume. The surface area and pore volume of sample 1001 was not measured.

Overall, all processing conditions result in a cryogel with a greater amount of pore volume than the bare silica. The bare silica was shown to have a total pore volume of 0.69 cm^3/g. Cryogel samples have pore volumes of anywhere from 0.91 to 1.68 cm^3/g. This constitutes an increase in pore volume of at least 37% and at most 266% over the bare silica. Among identically processed samples, 401 and 404, the pore volume varies from 0.83 – 1.4 cm^3/g. The high degree of variation of pore volume, as well as bulk density is very noticeable in freeze dried samples. Air dried samples, 502 and 504 differ by only 4.8 % and 4.9% in their volume and bulk density respectively. The somewhat random nature of particle suspension, freezing, and freeze drying techniques is a main reason for the large variability in absolute pore volume and bulk density, even between similarly processed samples. Freezing and freeze drying processes also appear to affect the macroscopic texture and bulk density compared to non-freeze dried samples.

Thermogravimetric Analysis

Temperature Regime: 100-200°C

Another primary method that was used to mete out the differences resulting from changes in processing conditions was thermogravimetric analysis. In this way, we can determine in general terms the overall surface chemistry of a given sample, which is important for any adsorption interactions or chemical reactions with the silica surface. As previously explained, weight loss from silica samples has been shown in previous literature to conform to three different temperature regimes: 100-200°C, 200-600°C, and 600-800°C, which correspond to the loss of physically adsorbed water, hydrogen bonded hydroxyl group condensation, and the partial loss of non-hydrogen bonded hydroxyl groups, respectively. Weight loss, as a percentage of total TGA sample weight, for each temperature range can be seen below in Figures 26 and later 27.

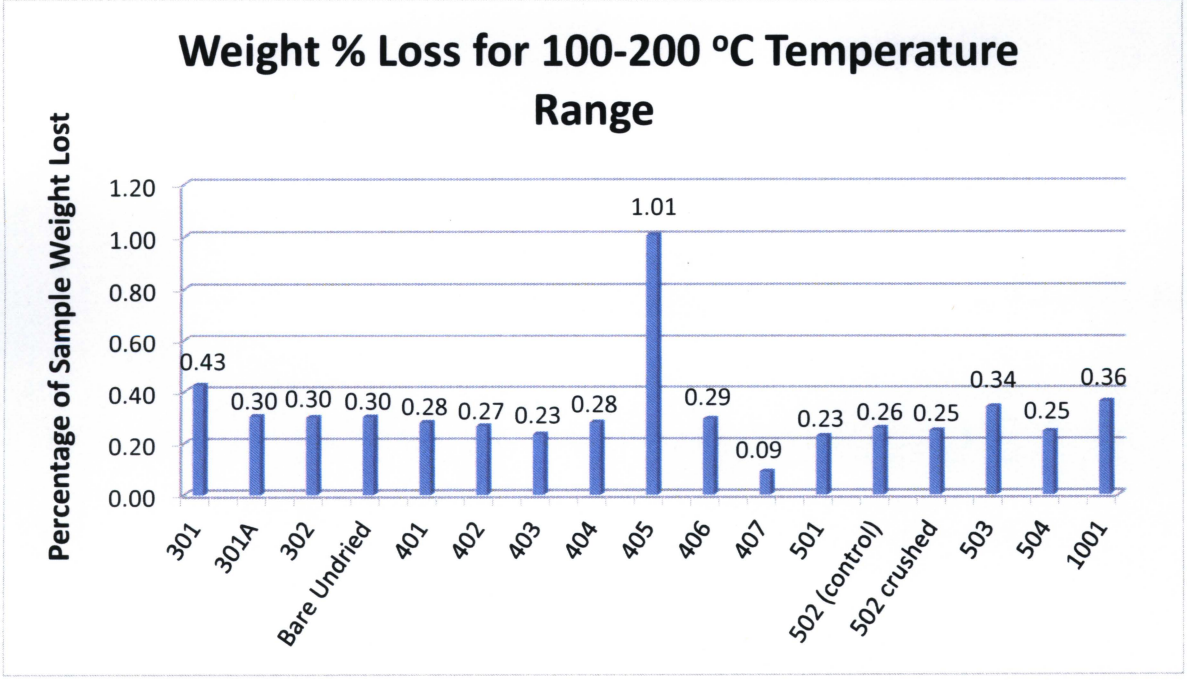

Figure 26. Weight loss as a percentage of total sample weight for cryogel samples between 100 and 200°C. Mainly adsorbed water is driven from the sample in this temperature range.

As seen in Figure 26, sample 405, the sample whose initial slurry was pH adjusted to 10, lost more than twice as much weight as any other sample in the 100-200 °C temperature range. Overall percentages for weight loss may seem low, with the highest weight loss being 1.01 wt % for sample 405, but recall that we are tracking the weight loss of surface groups and representing that loss as a portion of the total sample weight. If the silica in question did not have such a small particle size, and thus a high surface area to volume ratio, the magnitude of the weight loss would be even smaller. Keep in mind also that all samples were dried at 100°C for 3-4 hours before TGA measurements were taken. Therefore, the water evacuated in this temperature range is mainly water interacting with the surface of the silica, which increases its evacuation temperature.[5] For whatever reason, sample 405 seems to have more than twice as much adsorbed surface water as any other sample, even after heating at 100°C in preparation for TGA. As discussed previously, the surface area of sample 405 decreased significantly due to the high pH (10) of the initial slurry. Knowing this, one would assume that less water would be retained by sample 405, since water interacts mainly with the polar hydroxyl groups on the surface, and Si-O-Si (siloxane) groups are relatively hydrophobic. To illustrate the point: sample 405 has surface area of 172.4 m^2/g which is about 69% of the average of 275 m^2/g for other cryogel samples.

The isoelectric point of silica occurs at a pH of 1.7-3.5, and it follows that surface charge increases at high pH, above the isoelectric point.[24] Sample 405 was adjusted to pH 10 in the slurry stage, and therefore carried a higher surface charge in the slurry stage than any of the other samples, which were left at their unadjusted pH of ~4.5. More highly charged surfaces would naturally bond more strongly to water molecules than weakly charged surfaces, which may explain why sample 405 retained so much water even after drying at 100°C. However, it is unclear if this would be a valid explanation for the extra water retention, since the silica is no

longer suspended in water after freeze drying. Another possible explanation for the large amount of water in sample 405 would be that the water was trapped there. The rate of silanol condensation reactions increases at pH > 7, which likely contributed to the reduced surface area of sample 407.[21] This could have trapped water in the voids between particles as the silanol groups condensed, both from water resulting from the condensation reaction, as well as from solvent water trapped during the formation of siloxane bonds and bridges between primary particle surfaces. The trapped water could only then escape at temperatures between 100-200°C.

Another sample thought to have an altered surface chemistry is sample 407. The partial lack of hydroxyl groups discussed earlier may explain why only 0.09 wt% of water was evacuated from the sample in this temperature range. A lack of hydrophilic hydroxyl surface groups necessarily makes the silica surface more hydrophobic (more siloxanes or Si-O-Si groups), and therefore less likely to retain adsorbed water.[5] The next lowest weight loss for a cryogel in this temperature range was 0.23 wt% for sample 403 and 501. This could indicate that silica that has lost some of its surface hydroxyl groups cannot interact with or retain as much water as other samples. This would make sense since losing hydroxyl groups makes the silica surface more hydrophobic.[5]

Temperature Regime: 200-600°C

The 200-600°C temperature range has been established as the temperature regime in which hydrogen bonded hydroxyl groups are driven from the silica surface. Figure 27 shows the weight loss for this temperature range among all samples. A subset of the y axis was chosen to highlight the differences between each sample. To determine whether a sample lost significantly more weight than other samples, a pooled standard deviation was calculated. For the 200-600°C

range, the pooled standard deviation was calculated to be 0.0174 wt %, which equates to ~0.8% of total weight loss, depending on the sample. A t value was calculated for each combination of

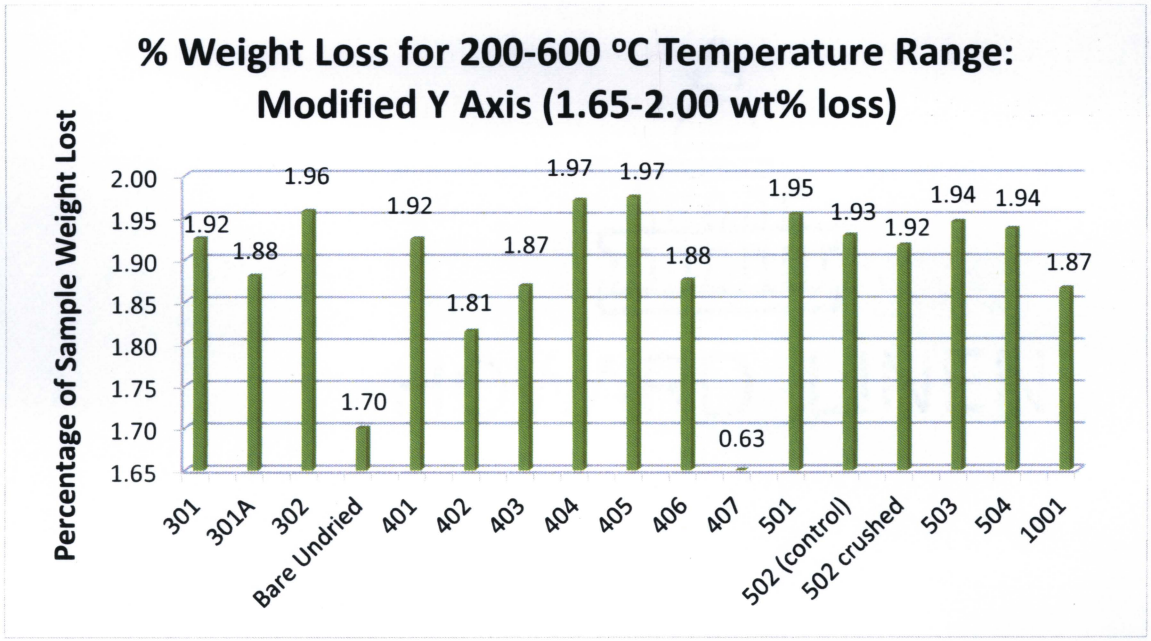

Figure 27. Weight loss between 200 and 600°C. Hydrogen bonded hydroxyl groups are driven from the surface in this temperature range.

samples based on the difference between their % weight loss in this temperature range. This was done according to equation 7 below. An example of an Excel table compiled to facilitate this

$$t_{calculated} = \frac{|x_1 - x_2|}{s_{pooled}} \sqrt{\frac{n_1 n_2}{n_1 + n_2}} \qquad (7)$$

comparison can be seen in Table 4. The calculated t values can be seen in tables 4, 5, and 6. The pooled standard deviation was calculated using three different samples with 4 measurements each, yielding 12 - 3 = 9 degrees of freedom. Therefore, at the 95% certainty level a standard t table shows the critical t value to be 2.262. Tables 4, 5, and 6 highlight the pairs of samples whose t values exceed this critical value. The weight loss between these pairs of samples can be

considered statistically significant with a 95% confidence level. A more in depth explanation of how to read tables 4, 5 and 6 follows below.

		404	**405**	**406**
3 wt % frozen 48 hrs	301	1.890	2.044	-2.014
3 wt% frozen 11 days	302	0.553	0.706	-3.352
plain fumed silica	Bare	18.637	18.791	14.733
larger sample, though not dried	Bare Undried	11.144	11.298	7.240
Normal 4 wt%	401	1.900	2.054	-2.004
sonicated 5 mins	402	6.406	6.560	2.502
sonicated 25 mins	403	4.188	4.341	0.283
pH 4.3	404	0.000	0.154	-3.904
pH 10	405	-0.154	0.000	-4.058
stirred 48 hours	406	3.904	4.058	0.000
heated 650 C 12 hrs	407	55.035	55.188	51.130
normal 5 wt %	501	0.698	0.852	-3.207
control not frozen or freeze dried	502 (control)	1.724	1.878	-2.180
crushed up chunks before TGA	502 crushed	2.221	2.374	-1.684
briefly frozen and freeze dried	503	1.069	1.223	-2.835
frozen 48 hrs and air dried	504	1.417	1.571	-2.487
10 wt%	1001	4.311	4.465	0.407

Table 4: Subset of sample comparison table for the 200-600°C temperature range. Each number denotes the t value considering the difference in % weight loss between the intersecting sample numbers at the head of the column and to the left of the row. Green denotes the column sample number lost significantly more weight than the intersecting row number. Red denotes the opposite.

The highlighted cells indicate a significant difference between samples. When read from the top down, the sample whose number is in bold at the head of the column is indicated to be either significantly different, or not significantly different than the sample in the left most column. For example, Table 4 indicates that sample **404** lost significantly more weight than sample **402** (row to the left) in the 200-600°C temperature range. The full significance table for the 200-600°C temperature range appears in tables 5 and 6. One important result for this temperature range is that all samples lost significantly more weight than the bare unmodified silica AND sample 407, which was heated to 650°C for a period of 12 hours prior to

cryogelation. In other words, all of our cryogel samples seem to contain more hydrogen bonded hydroxyl groups than the regular out-of-the-bag nanoparticulate silica, as well as sample 407. The results for weight loss in this temperature range based on processing conditions are itemized

	301	**401**	**501**	**1001**	407	**402**	**403**	**404**	**405**
301	0.000	-0.010	1.192	-2.421	-53.145	-4.516	-2.297	1.890	2.044
302	-1.337	-1.347	-0.145	-3.758	-54.482	-5.853	-3.635	0.553	0.706
Bare	16.747	16.737	17.939	14.326	-36.398	12.231	14.449	18.637	18.791
Bare Undried	9.254	9.244	10.447	6.833	-43.890	4.738	6.957	11.144	11.298
401	0.010	0.000	1.202	-2.411	-53.134	-4.506	-2.287	1.900	2.054
402	4.516	4.506	5.708	2.095	-48.629	0.000	2.218	6.406	6.560
403	2.297	2.287	3.490	-0.124	-50.847	-2.218	0.000	4.188	4.341
404	-1.890	-1.900	-0.698	-4.311	-55.035	-6.406	-4.188	0.000	0.154
405	-2.044	-2.054	-0.852	-4.465	-55.188	-6.560	-4.341	-0.154	0.000
406	2.014	2.004	3.207	-0.407	-51.130	-2.502	-0.283	3.904	4.058
407	53.145	53.134	54.337	50.723	0.000	48.629	50.847	55.035	55.188
501	-1.192	-1.202	0.000	-3.613	-54.337	-5.708	-3.490	0.698	0.852
502 (control)	-0.166	-0.176	1.026	-2.587	-53.310	-4.682	-2.463	1.724	1.878
502 crushed	0.331	0.321	1.523	-2.090	-52.814	-4.185	-1.967	2.221	2.374
503	-0.821	-0.831	0.371	-3.242	-53.966	-5.337	-3.119	1.069	1.223
504	-0.473	-0.483	0.719	-2.894	-53.618	-4.989	-2.771	1.417	1.571
1001	2.421	2.411	3.613	0.000	-50.723	-2.095	0.124	4.311	4.465

Table 5. Summary of weight loss statistics (t values with significant values highlighted) for the processing conditions of: solids loading, heat treatment, sonication, and pH adjustment.

	501	502	503	504	301	302
301	1.192	0.166	0.821	0.473	0.000	1.337
302	-0.145	-1.171	-0.516	-0.864	-1.337	0.000
Bare	17.939	16.913	17.568	17.220	16.747	18.084
Bare Undried	10.447	9.420	10.075	9.728	9.254	10.592
401	1.202	0.176	0.831	0.483	0.010	1.347
402	5.708	4.682	5.337	4.989	4.516	5.853
403	3.490	2.463	3.119	2.771	2.297	3.635
404	-0.698	-1.724	-1.069	-1.417	-1.890	-0.553
405	-0.852	-1.878	-1.223	-1.571	-2.044	-0.706
406	3.207	2.180	2.835	2.487	2.014	3.352
407	54.337	53.310	53.966	53.618	53.145	54.482
501	0.000	-1.026	-0.371	-0.719	-1.192	0.145
502 (control)	1.026	0.000	0.655	0.307	-0.166	1.171
502 crushed	1.523	0.497	1.152	0.804	0.331	1.668
503	0.371	-0.655	0.000	-0.348	-0.821	0.516
504	0.719	-0.307	0.348	0.000	-0.473	0.864
1001	3.613	2.587	3.242	2.894	2.421	3.758

Table 6. Summary to the data pertaining to freezing time, freeze drying, and freezing vs. not freezing processing conditions.

below. The data in the figures below show weight loss percentages, which were used to compute the t values shown in tables 5 and 6.

Solids Loading – Sample 301, 401, and 501 all lost similar amounts of weight from 200-600°C (Figure 28), while sample 1001 lost significantly less weight than many other samples, including

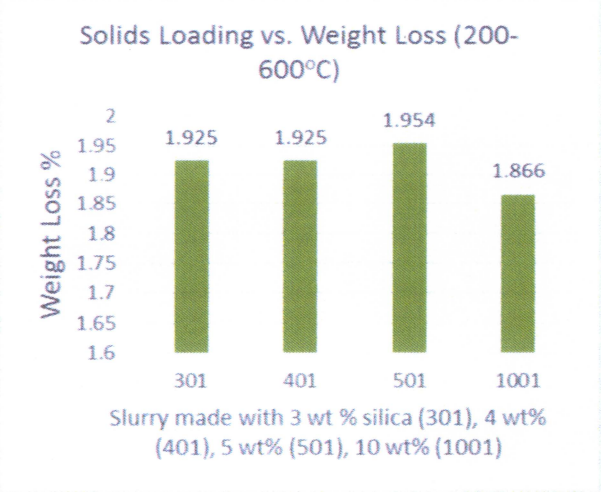

Figure 28. Graph detailing the weight loss of samples and solids loading of initial silica-water slurry.

301, 401, and 501. Weight loss in this temperature range indicates evacuation of hydrogen bonded hydroxyl groups. As discussed previously, hydrogen bonding between surface hydroxyl groups occurs mainly between groups on different particles, rather than the same particle. Sample 1001 loses less weight in this temperature range than other, lower weight % samples, likely indicating a lower amount of particle-particle contact. This trend is also present in bulk density measurements shown earlier in the text. Perhaps differences in particle dispersion during slurry manufacture and freezing are the cause.

Sonication – The sonicated samples, 402 and 403, lost less weight in this temperature range than all other samples except 407 and the bare silica (Figure 29). Sonicated samples may have been dispersed more completely than other samples, resulting in a lower amount of particle-particle contact. The possible role particle-particle contact plays in evacuation of hydrogen bonded hydroxyl groups will be explained after processing condition itemization.

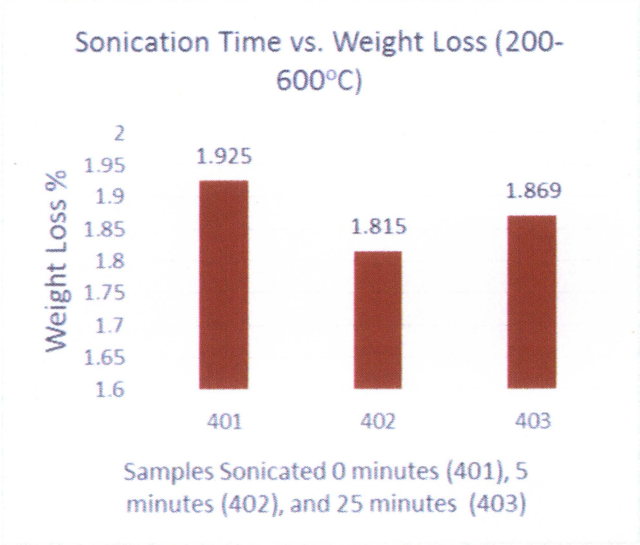

Figure 29. Graph comparing the sonication time of samples to weight loss.

pH Adjustment – Sample 404 exhibited relatively high weight loss in this range. 405 exhibited a similarly high relative weight loss, despite its significantly reduced surface area (Figure 30). Sample 404 also lost significantly more weight than sample 401, which was processed identically. This could point to a significant variation in weight loss among similarly processed samples. Considering the variation in bulk density and pore volume in freeze dried samples, this would not be unreasonable.

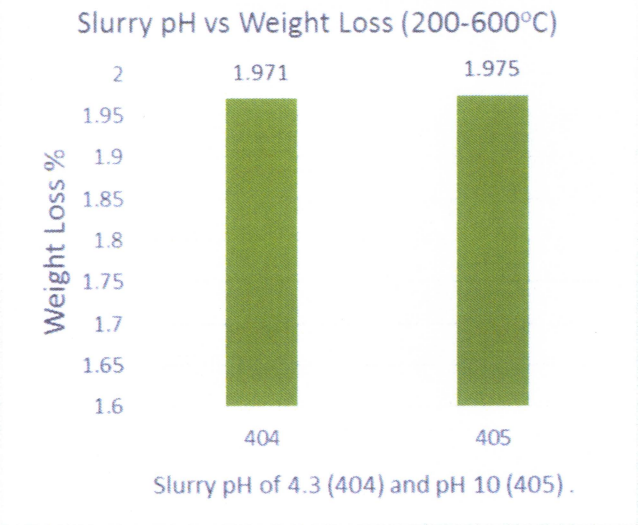

Figure 30. Graph detailing weight loss of 404 (pH 4.3) and 405 (pH 10)

Heat Treatment – Sample 407 (silica heated to 650°C before cryogelation) exhibited the least weight loss in this temperature region by far, even losing less weight than the bare silica sample (Figure 31). This piece of evidence servers to confirm the dehydroxylated state of the silica surface in this sample. By extension, the silica surface was not re-hydroxylated upon exposure to water during cryogel preparation.

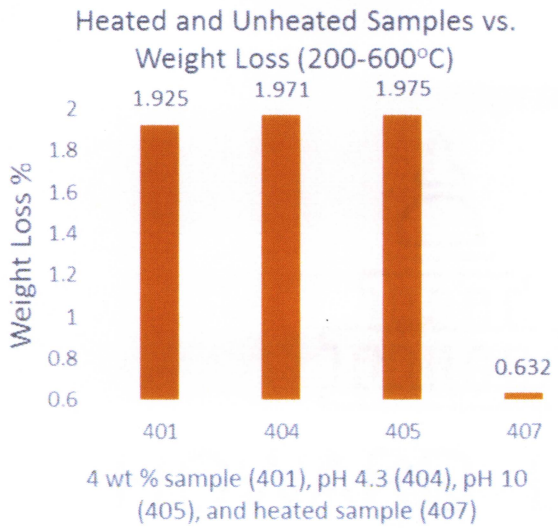

Figure 31. Graph comparing the weight loss of heated sample 407, and other samples whose silica was not heated prior to cryogel manufacture.

Freezing Time – Sample 302 (frozen 11 days) lost slightly more weight from 200-600°C than sample 301 (frozen 48 hours) (Figure 32). The difference in weight loss between 301, 301A (frozen 72 hours) and 302 is not significant according to the established criteria. Previously, a trend of decreasing bulk density with increasing freezing time was shown to exist. No such trend is present when comparing weight loss and freezing time.

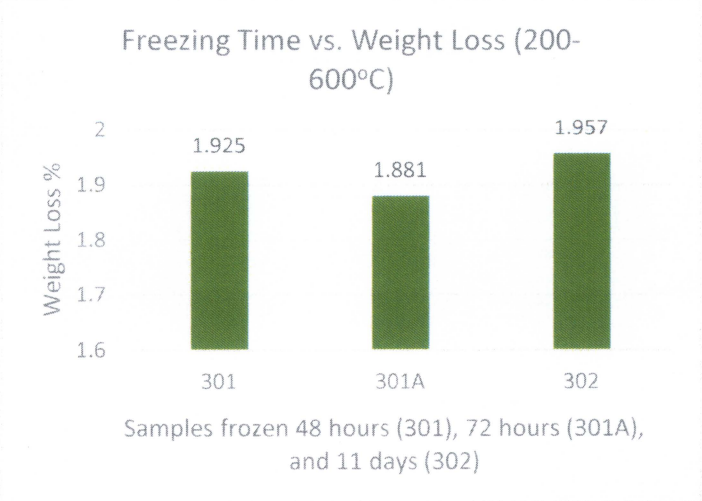

Figure 32. Graph comparing weight loss and freezing time.

Freezing vs. Not Freezing – Freezing did not seem to increase weight loss in this temperature regime compared to unfrozen samples (Figure 33). Specifically, sample 502, which was not frozen nor freeze dried, had the same weight loss profile as sample 504, which was frozen and air dried.

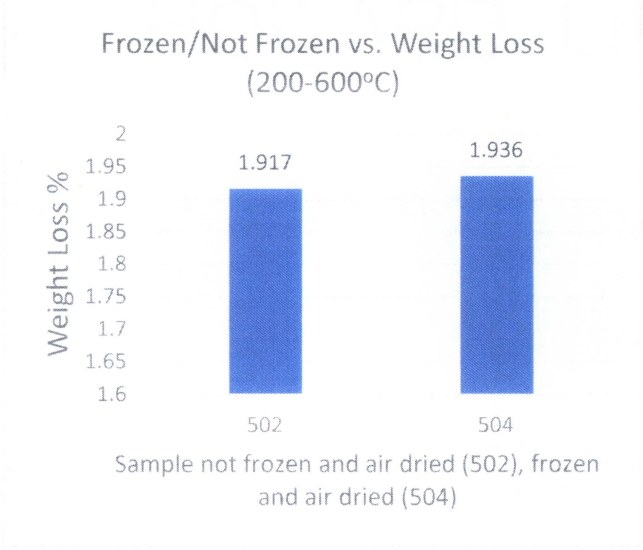

Figure 33. Graph comparing a sample that was not frozen prior to air drying, and a sample that was frozen for 48 hours prior to air drying.

Freeze Drying vs. Air Drying – Freeze dried samples exhibited no significant difference in weight loss in this temperature regime over samples that were not freeze dried (Figure 34). Samples 502 (not frozen or freeze dried) and 504 (frozen and air dried) were not significantly different from each

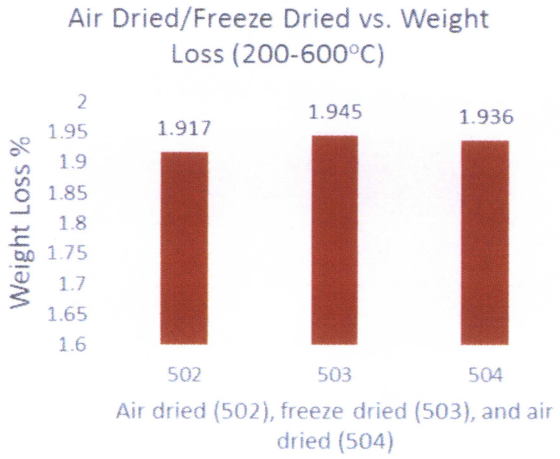

Figure 34. Graph comparing the weight loss of freeze dried (503) and air dried (502, 504) samples

other. The weight loss for sample 503, the briefly frozen and freeze dried sample, was slightly higher than samples 502 and 504, but this was not significant according to the established criteria.

It has been shown that individual hydroxyl groups groups on the silica surface are either isolated from one another completely, or weakly interacting with other nearby hydroxyl groups.[18] In other words, almost no close hydrogen bonding interaction occur between hydroxyl groups on the same surface. In the case of fumed silica, a hydroxyl group must interact with a hydroxyl group from the surface of another silica nanoparticle in order to undergo hydrogen bonding interactions. It would make sense that the more densely packed the primary silica nanoparticles are, the more hydrogen bonded hydroxyl groups should be present. The amount of weight loss from 200-600°C should therefore be an indication of how much close particle-particle interaction is present in a given sample. How then, does bulk density affect weight loss in cryogel samples? A higher bulk density should mean more closely packed particles, but bulk density depends on many factors, including packing of agglomerates, aggregates, secondary aggregates, etc. Bulk density might not accurately reveal how closely individual silica nanoparticles interact.

Additionally, the bulk density of the cryogel powders only reaches 0.344 g/cm^3 in the densest samples, which is only about 16% of the density of amorphous silica (2.2 g/cm^3), and 21% of the maximum theoretical powder density based on close packed spheres. Close packed spheres can obtain a theoretical density 74% of the maximum density. Since the powders are not very compact overall, interaction between particle surfaces is not as highly pronounced as it could be. When weight loss from 200-600°C is plotted vs. bulk density in Figure 35, we see that there seems to be some correlation between those two parameters. In addition to the reasons explained above, the presence of adsorbed water could also explain the somewhat low correlation between bulk density and weight loss. Layers of adsorbed water could have interfered with direct interaction between different particle surfaces and surface groups.

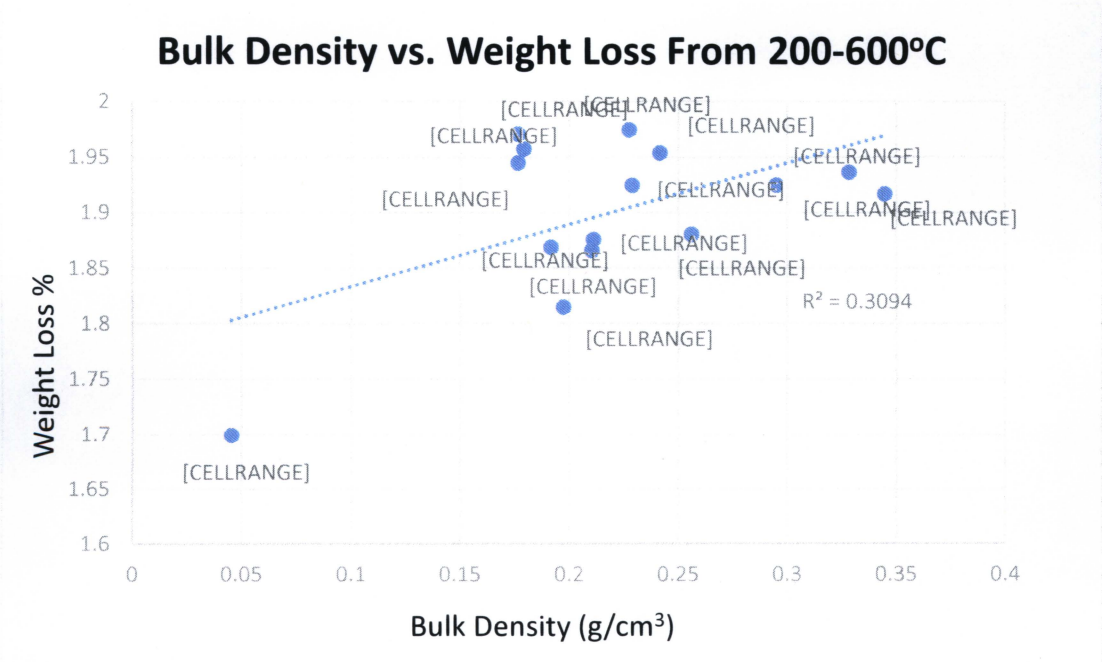

Figure 35. Bulk density vs. weight loss for all samples in the 200-600°C temperature range. Sample 407 was discounted as an outlier due to its unique processing conditions

Another assessment of the extent of particle packing could be pore volume, since a larger pore volume with r < 40nm should mean closer particle-particle interaction. But Figure 36,

which plots pore volume against weight loss from 200-600°C, shows no correlation between weight loss and pore volume in this temperature regime. If the amount of hydrogen bonded hydroxyl groups did increase appreciably with bulk density and pore volume, one would expect to see a larger weight loss the larger the bulk density, or measurable pore volume, of the sample. This is not the case here. The literature has shown that hydroxyl groups on the same surface either do not interact, or interact very weakly.[25] As such, hydrogen bonding interaction must

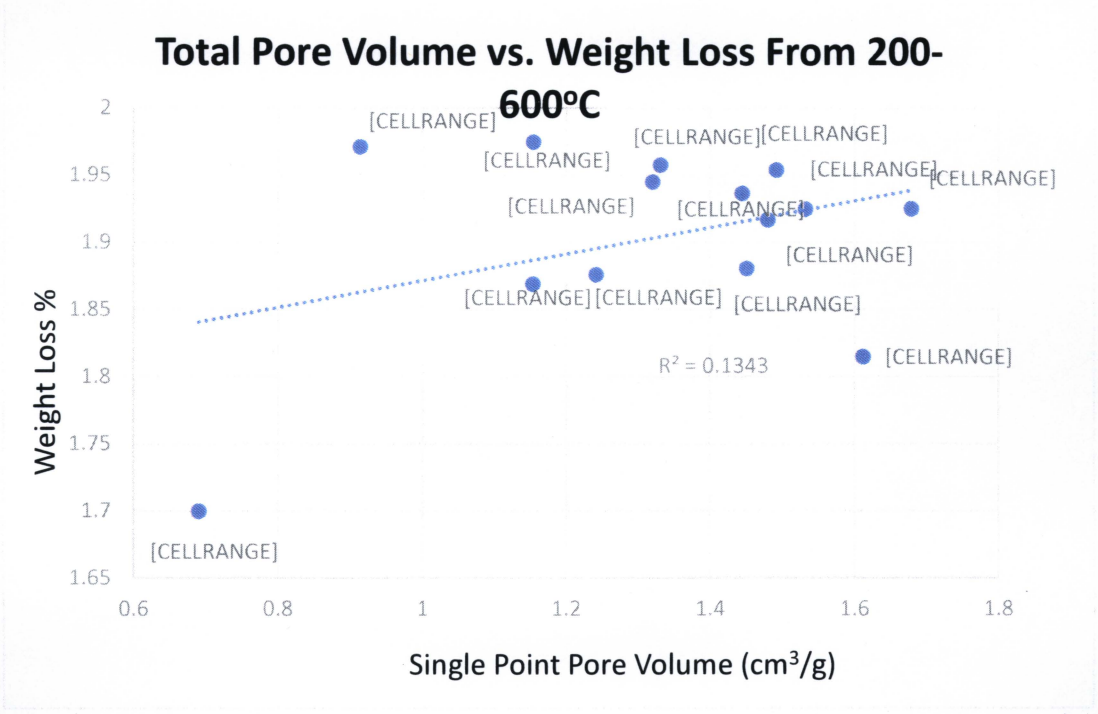

Figure 36. Pore volume plotted vs. weight loss from 200-600°C. Sampl 407 was discounted as an outlier due to its unique processing conditions.

come from hydroxyl groups on a nearby silica surface. Since no positive correlation is observed between bulk density and weight loss, or pore volume ($r < 40$ nm) and weight loss, one can conclude that these properties are not a good measure of particle-particle interaction.

Regardless of the variations in weight loss between processed samples, all samples (with the exception of sample 407, the heated sample) show a significantly different weight loss from

200-600°C compared to the bare, unprocessed silica. It is known that fumed silica is imparted with some surface hydroxyl groups as it is produced, and can achieve a greater degree of hydroxylation equal to no more than 4.6-4.9 hydroxyl groups per 100 $Å^2$.[1,8,5] The TGA experiments performed in this study reflect this trend, with processed samples losing more weight from 200-600°C than the bare silica. It seems logical to say that any difference in weight loss, and therefore hydrogen-bonded hydroxyl group content, is due to one or more of the processing conditions applied. Only sample 407 loses less weight from 200-600°C than the bare sample, due to the heating at 650°C before processing. This confirms our suspicion that the surface has been partially de-hydroxylated, especially with respect to hydrogen bonded hydroxyl groups. Moreover, the surface was not re-hydroxylated and remains less hydroxylated relative to the bare unprocessed silica. More specifically, the bare silica sample exhibited a weight loss 3 times larger than sample 407 in this temperature range. Sample 405 lost the most weight from 200-600°C, and this constitutes an increase of ~16% (as in 1.16 times, not 16 wt %) over the bare sample. Exempting sample 407 and the bare silica, the maximum variation in weight loss between processed samples becomes ~8%. While easily measureable and perhaps significant, weight loss in all samples (407 excluded) varies proportionally much less than bulk density or pore volume. Both pore volume and bulk density varied by a factor of ~2 between the highest and lowest measurements, with 407 and the bare sample excluded. Most processing conditions seem to affect the morphology of the sample more than the amount of hydroxyl groups driven off upon heating.

The pooled standard deviation in the 200-600°C range was calculated to be 0.0174 wt %, which equates to ~0.8% of total weight loss, depending on the sample. What this means is that weight loss *within a given sample* varies little between TGA measurements. This standard

deviation does not take into account possible variations in sample consistency resulting from freezing and freeze drying. Sample 401 and 404 were prepared in almost exactly the same fashion, but differed significantly on several fronts, though not in weight loss from 200-600°C. The only difference is that the pH of sample 404 was measured before freezing and freeze drying, which may have introduced a small amount of KCl via the pH meter electrolyte solution. Samples 401 and 404 exhibit dissimilar bulk density and pore volume, which is shown in Table 7. It is apparent that some caution must be used when drawing conclusions from some of

	Bulk Density (g/cm^3)	Pore Volume (cm^3/g)	Weight Loss % 200-600°C
401	0.228	1.396	1.925
404	0.176	0.827	1.971
502	0.344	1.516	1.917
504	0.328	1.446	1.936

Table 7. Bulk density, pore volume, and weight loss of hydrogen-bonded hydroxyl groups for selected samples.

the variations in cryogel properties, as differences between samples could be due to processing conditions or the freezing/freeze drying process. In contrast, samples 502 and 504, which were not freeze dried, differ by less than 5% from one another in both their bulk density and pore volume. This seems to indicate that freeze drying in particular imparts a variability in the bulk density and pore volume of samples. Additional work could be done to further investigate the consistency of the effects of freeze drying on sample morphology.

A more in depth explanation of particle-particle interaction may shed more light on the variations in weight loss and hydroxyl group interaction. Primary silica nanoparticles interact with one another via hydrogen bonding between surface hydroxyl groups.[26] A diagram of this phenomenon is shown in Figure 37. CAB-O-SIL products, like the one used in this study are normally used to impart viscosity control and other favorable properties to coatings or other

liquid based systems. This is achieved by the formation of a particle network formed via inter-particle hydrogen bonding action.[26] Forces applied during the application of a coating or other silica suspension break the weak hydrogen bonds between particles and allow the coating to

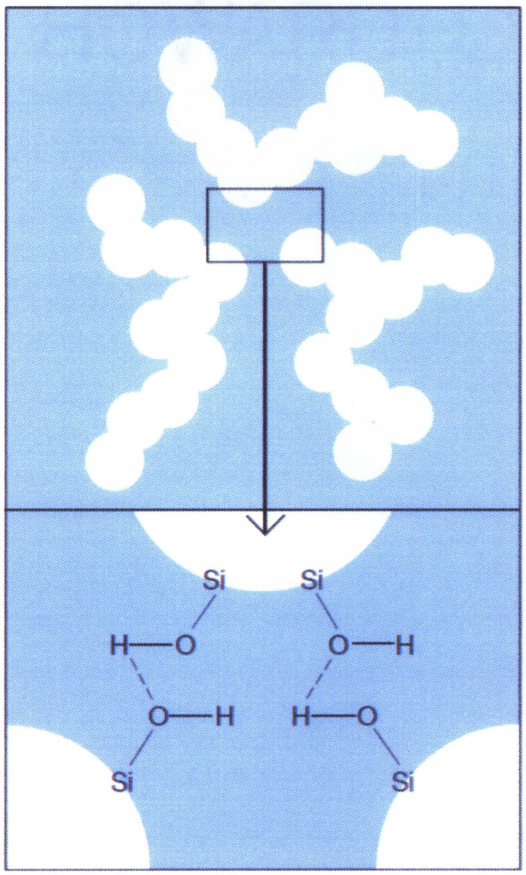

Figure 37. Diagram showing the possible hydrogen bonding interactions between the surface groups of silica nanoparticles. Interaction with polar solvents can disrupt particle-particle interaction.[26]

uniformly deposit on the surface. The silica nanoparticle network quickly reforms in the absence of any outside forces, restoring viscosity to the system. This process is mainly intended to take place in a non-polar medium. Polar components or solvents can disrupt or take precedence over the hydrogen bonding interaction between particle surface groups.[26] Since this study involves suspension of silica particles in water, a very polar solvent, the silica particle network is more likely to be disrupted.

As mentioned earlier, it would be logical that high bulk density should lead to a greater incidence of interaction between surface hydroxyl groups. This would in turn result in a higher proportion of hydrogen bonded hydroxyl groups. While hydrogen bonding between surface groups certainly can occur, hydrogen bonding between surface groups and water molecules seems far more likely in aqueous suspension given the high water concentration.[26] This would explain why the data presented shows no consistent correlation between the number of hydrogen bonded hydroxyl groups and bulk density/pore volume. Additionally, greater dispersion of silica nanoparticles, which may be caused by sonication or stirring, should further increase the amount of water-surface interaction.

It seems likely that enough water would remain in the sample to interfere with particle-particle surface group interactions even after drying at 100°C. Water molecules interacting with the surface of silica are not completely driven off until around 190°C.[5] The data presented would seem to confirm this, since all cryogel samples exhibited measurable weight loss from 100-200°C. If a higher amount of interaction between the surface groups of different particles and/or more hydrogen bonded hydroxyl groups is desired, dispersion and compaction in a non-polar solvent may be desirable. According to Cabot Corporation, the viscosity changing effects of CAB-O-SIL fumed silica will remain active as long as the solvent/suspension molecules contain multiple hydrogen bonding sites which is consistent with the idea that a non-polar medium would result in increased nanoparticle interactions.[26]

Temperature Regime: 600-800°C

The last set of TGA data to report is the weight loss for samples in the 600-800°C temperature range, in which non-hydrogen bonded hydroxyl begin to be driven from the silica surface. Figure 38 shows the weight loss for all samples in this temperature range. One will

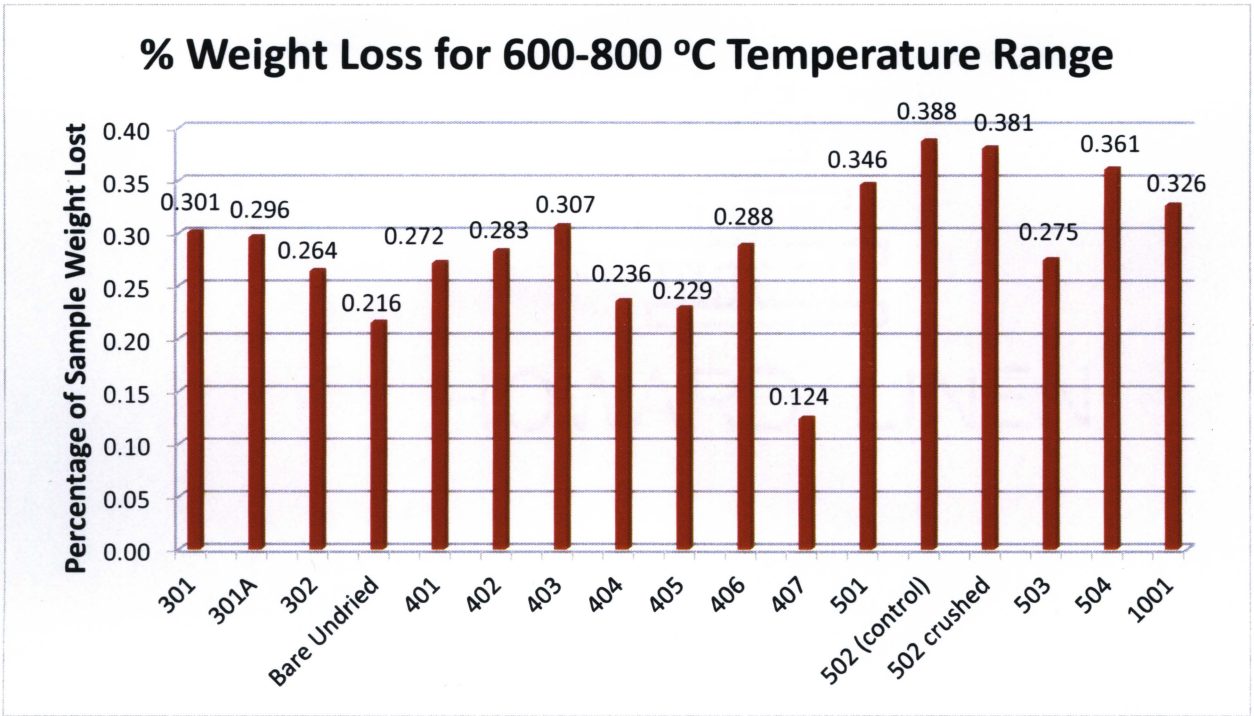

Figure 38. Weight loss for the 600-800°C temperature range. Non-hydrogen bonded hydroxyl groups start to evacuate at 600°C. Excluding the bare sample and 407, weight loss varies by 0.159 wt%. This constitutes a variation of 69% of the lowest weight loss measurement.

notice that the weight loss for sample 407 was significantly less than all other samples, including the bare sample. It makes sense that some of the non-hydrogen bonded hydroxyl groups would be gone since the sample was heated to 650°C for a significant length of time. The average weight loss percentage from 600-800°C (~0.3 wt %) is several fold less than the average weight loss from 200-600°C (~1.8 wt %) for other cryogels. This is also not unexpected due to the small temperature range (200°C vs. 400°C) as well as the fact that non-hydrogen bonded hydroxyl groups can persist on the silica surface even at 1000-1100°C, though these are a significant distance from one another.[5] It is not the purpose of this study, nor is it possible with the experiments conducted to determine exactly how many hydroxyl groups of each type exist on the sample surface. More formal studies on the precise number of hydroxyl groups on a maximally hydrated silica surface give 1.4 +/- 0.1 non-hydrogen bonded hydroxyl groups and 3.2 +/- 0.1

hydrogen bonded hydroxyl groups per 100 Å^2.[27] TGA data appears to spot general trends, such as de-hydroxylated state of sample 407, or the smaller than average weight loss of stirred, sonicated samples. A subset of the significance table for the differences in weight loss % from 600-800°C is shown below in Table 9.

		301	302	Bare Undried	401	402	403	404	405
3 wt % frozen 48 hrs	301	0.000	-0.922	-2.147	-0.730	-0.449	0.152	-1.642	-1.811
3 wt% frozen 11 days	302	0.922	0.000	-1.225	0.192	0.472	1.073	-0.721	-0.890
bare though not dried	Bare Undried	2.147	1.225	0.000	1.417	1.697	2.299	0.505	0.336
Normal 4 wt%	401	0.730	-0.192	-1.417	0.000	0.281	0.882	-0.912	-1.081
sonicated 5 mins	402	0.449	-0.472	-1.697	-0.281	0.000	0.601	-1.193	-1.362
sonicated 25 mins	403	-0.152	-1.073	-2.299	-0.882	-0.601	0.000	-1.794	-1.963
pH 4.3	404	1.642	0.721	-0.505	0.912	1.193	1.794	0.000	-0.169
pH 10	405	1.811	0.890	-0.336	1.081	1.362	1.963	0.169	0.000
stirred 48 hours	406	0.316	-0.605	-1.831	-0.414	-0.133	0.468	-1.326	-1.495
heated 650 C 12 hrs	407	4.444	3.522	2.297	3.714	3.995	4.596	2.802	2.633
normal 5 wt %	501	-1.143	-2.064	-3.289	-1.873	-1.592	-0.991	-2.785	-2.954
control not frozen or freeze dried	502 (control)	-2.185	-3.107	-4.332	-2.915	-2.635	-2.034	-3.827	-3.996
crushed up chunks before TGA	502 crushed	-2.016	-2.938	-4.163	-2.746	-2.465	-1.864	-3.658	-3.827
briefly frozen and freeze dried	503	0.656	-0.266	-1.491	-0.074	0.207	0.808	-0.986	-1.155
frozen 48 hrs and air dried	504	-1.512	-2.434	-3.659	-2.242	-1.962	-1.360	-3.154	-3.323
10 wt%	1001	-0.647	-1.568	-2.794	-1.377	-1.096	-0.495	-2.289	-2.458

Table 9. Subset of the table highlighting significant differences between samples from 600-800°C. Highlighted comparisons fall outside the range of possible measurement error with a 95% confidence level.

Sonication – Samples 402 and 403 did not lose significantly more weight in this temperature range than most other samples save and 407.

pH adjustment – Sample 405 appeared to be very similar to sample 404 in weight loss. These two samples did not lose significantly more weight than the bare sample.

Air dried samples – Samples 502 and 504 stand out in this temperature range as losing significantly more weight than several samples, 502 especially. Note that samples 504 and 502 exhibited similar weight loss from 200-600°C (~1% variation) and 600-800°C (5.5% variation).

	406	407	501	502	502 crushed	503	504	1001
301	-0.316	-4.444	1.143	2.185	2.016	-0.656	1.512	0.647
302	0.605	-3.522	2.064	3.107	2.938	0.266	2.434	1.568
Bare Undried	1.831	-2.297	3.289	4.332	4.163	1.491	3.659	2.794
401	0.414	-3.714	1.873	2.915	2.746	0.074	2.242	1.377
402	0.133	-3.995	1.592	2.635	2.465	-0.207	1.962	1.096
403	-0.468	-4.596	0.991	2.034	1.864	-0.808	1.360	0.495
404	1.326	-2.802	2.785	3.827	3.658	0.986	3.154	2.289
405	1.495	-2.633	2.954	3.996	3.827	1.155	3.323	2.458
406	0.000	-4.128	1.459	2.501	2.332	-0.340	1.828	0.963
407	4.128	0.000	5.587	6.629	6.460	3.788	5.956	5.091
501	-1.459	-5.587	0.000	1.043	0.873	-1.799	0.369	-0.496
502 (control)	-2.501	-6.629	-1.043	0.000	-0.169	-2.841	-0.673	-1.539
502 crushed	-2.332	-6.460	-0.873	0.169	0.000	-2.672	-0.504	-1.369
503	0.340	-3.788	1.799	2.841	2.672	0.000	2.168	1.303
504	-1.828	-5.956	-0.369	0.673	0.504	-2.168	0.000	-0.865
1001	-0.963	-5.091	0.496	1.539	1.369	-1.303	0.865	0.000

Table 10. Continued significance tables for the 600-800°C temperature range. Highlighted values correspond to t differences which are at a >95% confidence level of being statistically significant.

Heat Treatment – 407 also loses the least weight in this temperature range, even less than the bare sample. This serves to confirm that some non-hydrogen bonded hydroxyl groups were lost upon the initial heating at 650°C before the slurry stage.

Solids Loading – 501 and 1001 lost the most weight in this temperature range among 301, 401, 501, and 1001 samples.

To make any more sense out of the weight loss data, it is again necessary to compare weight loss to another metric such as bulk density. Unlike the weight loss for the 200-600°C range, bulk density actually did show a somewhat positive correlation with weight loss from 600-800°C, which is shown below in Figure 39. One could imagine, from a theoretical

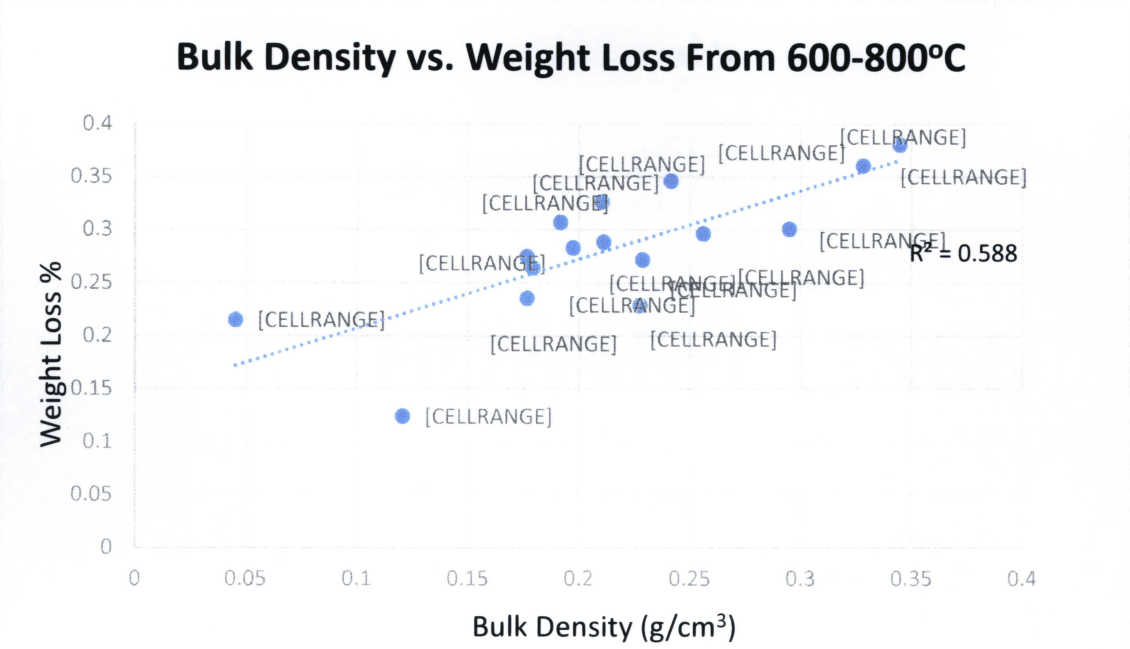

Figure 39. Weight loss % vs. bulk density graph for all samples showing a positive correlation between bulk density and weight loss in the 600-800°C temperature range.

standpoint, that an increase in bulk density might result in an increased amount of hydrogen bonded hydroxyl groups due to interactions between the surface groups of different particles (though water was shown to interfere with this possible mechanism). For non-hydrogen bonded hydroxyl evacuation from 600-800°C, no such mechanism comes to mind that might explain the increase in weight loss with bulk density. This correlation may simply be a coincidence, especially considering the fact that only a portion of the non-hydrogen bonded hydroxyl groups have been evacuated at 800°C. The main points are that air dried samples stood out in terms of weight loss, and that the bare sample was much closer to cryogel samples in terms of weight loss than in other temperature ranges.

Nuclear Magnetic Resonance

As mentioned in the introduction, NMR can be used to probe the chemical environment of the silica surface. Leonardelli et el. described the types of chemical environments present on

hydroxylated silica surfaces as follows, with Figure 40 illustrating different structures present on the silica surface and their corresponding resonances:[17]

Q2: and $Si(O_{0.5})_2(OH)_2$ the geminal (double) hydroxyl silanol groups (-90 ppm)

Q3: $Si(O_{0.5})_3OH$ the single hydroxyl silanol groups (-100 ppm)

Q4: $Si(O_{0.5})_4$ the siloxane groups which form the bulk of the material (-110 ppm)

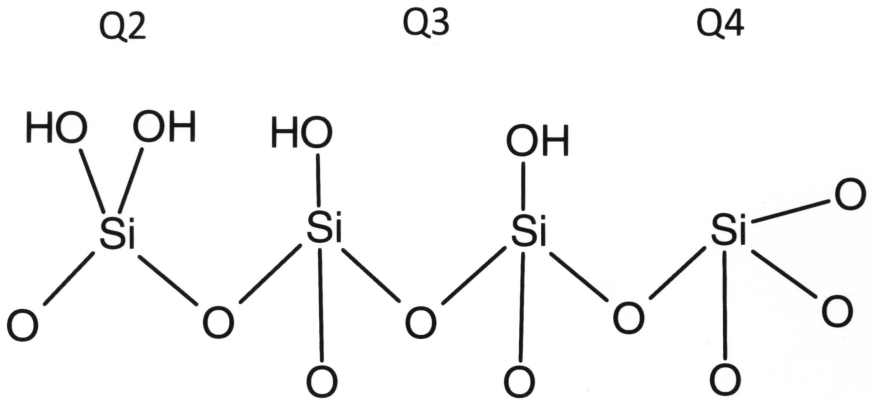

Figure 40. Shows the structure of various surface groups, Q2 (diol) at -90 ppm, Q3 (single silanol) at -100 ppm, and Q4 (siloxane) at -110 ppm.

According to the cited study the chemical shifts associated with each type of group are -91 ppm (Q^2), -100 ppm (Q^3), and -110 ppm (Q^4).[17] An important distinction to make is the difference between hydrogen bonded and non-hydrogen bonded hydroxyl groups vs. single and geminal hydroxyl surface groups. Aforementioned techniques such as IR spectroscopy and TGA are able to differentiate between hydrogen bonded and non-hydrogen bonded hydroxyl groups. NMR in contrast is capable of detecting silicon atoms with either one or two hydroxyl groups are attached. To be clear, the Q3 designation refers to silicon atoms in which three of the four spots in the silicon tetrahedra take part in Si-O-Si bonds, and the other spot is occupied by an –OH

group. In Q2 sites, two –OH groups occupy the same Si atom, and the remaining two sites are part of the bulk Si-O-Si bonds. It should be noted that geminal hydroxyl groups do not interact with each other via hydrogen bonding. In fact, most single surface hydroxyl groups do not interact at all, or only interact weakly with one another.[5] This NMR analysis cannot provide information on the relative amounts of hydrogen bonded vs. non-hydrogen bonded hydroxyl groups. However, NMR can still provide a rough comparison between the total amounts of hydroxyl groups on each sample and whether they are single or geminal hydroxyl groups.

Solid state ^{29}Si NMR measurements were taken for three samples: 401, 405, and the bare sample. As a reminder, 401 is a normal frozen and freeze dried 4 wt% sample, 405 was adjusted to pH 10 in the slurry stage, and the bare sample is just the CAB-O-SIL fumed silica straight from the manufacturer. The overlapped NMR spectra are shown below in Figure 41. To clarify, the leftmost peak corresponds to Q2, or the geminal hydroxyl silanol groups; the middle peak corresponds to Q3, or the single hydroxyl silanol groups; and the rightmost peak corresponds to Q4, or the bulk siloxane (Si-O-Si) groups. The scaling of the signal intensity between different NMR runs is not directly comparable, even between runs of the same sample. Proportions of different peaks in the same spectrum should remain the same when running the same sample twice. In analyzing and comparing our different NMR spectra, some kind of standard must be employed in order to extract any information on the relative amount of Q2, Q3, and Q4 groups present. The most constant factor in each sample would most likely be siloxane groups that make up the bulk of the material, which is represented by the Q4 signal. Therefore, the 3 NMR spectra are normalized according to the Q4 (siloxane) signal. In this way, a comparison of samples highlights some significant differences between spectra.

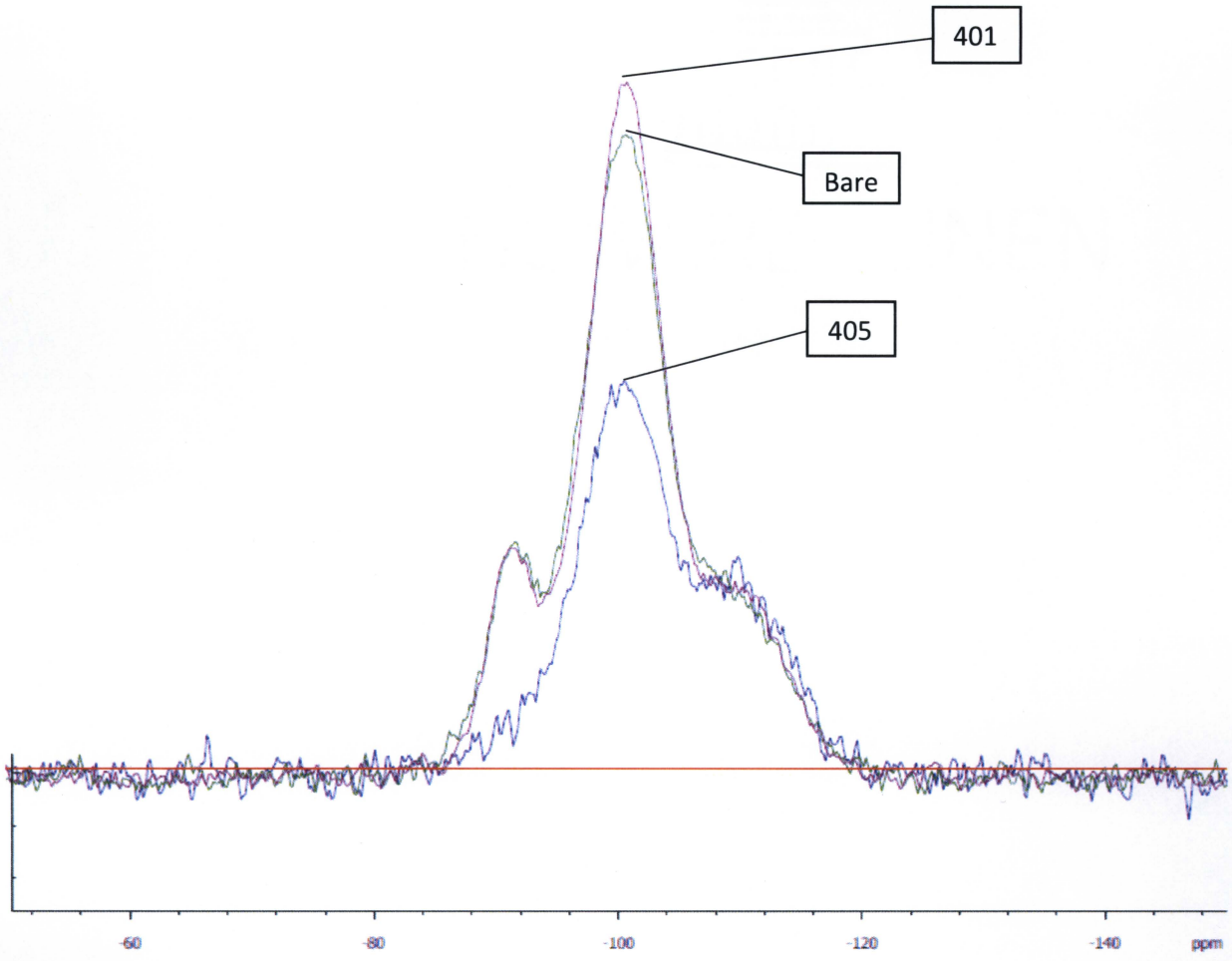

Figure 41. Comparison of the three NMR spectra for sample 405, 401, and the bare sample. Spectra were scaled so that the rightmost peak, which corresponds with the bulk siloxane (Si-O-Si). It was assumed that the siloxane peak would be roughly equal among all samples. Image created using GSim NMR Viewing/Processing Tool © Vamid Sorin 2008-2013

Precise peak shifts as calculated by the deconvolution program NUTS are as follows: Q2 at -91.0 ppm, Q3 at -100.6 ppm, and Q4 at -111.1 ppm. Sample 401 has a higher Q3 peak, corresponding to single silanol groups than either the bare sample or 405. Since these spectra are normalized to the Q4 signal intensity this suggests that sample 401 contains more single silanol groups than the bare sample. This supports earlier TGA data which shows that the silica surface of the cryogel samples is more hydrated than the bare silica. In contrast, the bare sample and 401

NMR spectra both have a Q2 peak around -90 ppm, corresponding to geminal silanols, with a very similar intensity. This indicates the bare sample and 401 have a similar number of geminal hydroxyl groups.

Sample 405 experienced a decrease in surface area since its slurry was adjusted to pH 10. Lower surface area results in fewer available sites overall, since hydroxyl groups must attach to a terminal Si atom. The underlying mechanism for the reduction of surface area is the large increase in solubility of silica in water at a pH > 10 and a subsequent re-deposition of the dissolved silica into the crevices between primary particles. Whether or not this affects the type of surface hydroxyl groups (non-hydrogen bonded/hydrogen bonded or single/geminal) is not clear, especially since the weight loss % from 200-600°C of sample 405 (pH 10) was not especially unique. Reactions involving silanols, which include simple Si-OH groups, have been analyzed by Iler and Brinker since they are a key factor in sol gel chemistry, among other things.[1,21] Equation 8 demonstrates the condensation/hydrolysis reaction that can occur between two silanol groups.[21]

$$\equiv Si - OH + HO - Si\equiv \underset{\text{hydrolysis}}{\overset{\text{water condensation}}{\rightleftharpoons}} \equiv Si - O - Si\equiv + H_2O \qquad (8)$$

The condensation reaction has been shown by Brinker, who cites Pohl and Osterholtz as a part of his analysis, to be acid and base catalyzed.[21,28] In addition, the reverse reaction of equation 7, hydrolysis of the siloxane Si-O-Si bond, is very slow, and may in fact be irreversible in certain cases.[21,28] This condensation action may have contributed to the low hydroxyl group content in sample 405 as characterized by NMR. Other samples would not have experienced with

phenomenon nearly as strongly as sample 405 since their slurries maintained a pH of ~4.3, where the rate of the silanol condensation reaction is slow. It should be noted that the surface of the CAB-O-SIL nanoparticulate silica does not contain alkylsilanetriol groups, which Brinker, Pohl and Osterholtz used in their studies. However, triply hydroxylated silicon atoms need not be present for the condensation reaction to occur. The extremely low level of geminal hydroxyl sites in sample 405, shown in Figure 40, may indicate that geminal hydroxyl sites undergo condensation reactions more readily than singly occupied sites.

Equations 9, 10, and 11 cover the possible reactions between different silanol groups, whether single or geminal. In Equation 8, a single and a geminal hydroxyl group

$$Si(OH)_2 + SiOH \rightarrow Si\text{-}O\text{-}Si + SiOH + H_2O \quad (9)$$

$$2\ Si(OH)_2 \rightarrow 2\ SiOH + 2\ Si\text{-}O\text{-}Si + 2\ H_2O \quad (10)$$

$$2\ SiOH \rightarrow Si\text{-}O\text{-}Si + H_2O \quad (11)$$

react to form a siloxane and a single hydroxyl group. This reaction would result in the reduction of the Q2 signal in NMR analysis, since the geminal hydroxyl group is gone. The Q3 signal would remain the same, since one single hydroxyl group is present before and after the reaction. In the case of equation 9, two geminal silanols come together, and one silanol from each geminal group reacts to give a siloxane bond and two single silanol groups. The Q2 signal would decrease since two geminal groups are eliminated, and the Q3 signal would actually increase, since two new single hydroxyl formations have emerged. Lastly, equation 10 denotes the reaction of two single silanol groups, which would only result in a decrease in the Q3 signal. Since the Q2 peak of the NMR spectrum for sample 405 is lower than that of other samples, we may conclude that some combination of processes 8 and 9 have occurred during the reduction of surface area at pH 10. Since the Q3 signal for sample 405 is also reduced compared to other

samples, we may conclude that process 10 took place as well. More significantly, process 10 occurred more often during the reduction of surface area than process 9. Processes 9 and 10 compete by increasing and decreasing the amount of single silanol groups (Q3) respectively. Since the Q3 signal is lower in sample 405, process 10 must occur more often than process 9. The reason single silanols appear to react more often, as in process 10, may be that there are simply more single silanol groups. Previous research estimates the geminal hydroxyl group content to be no more than 30%.[20] Table 11 compares the deconvoluted peak area, obtained by using the NUTS deconvolution software by Acorn NMR Inc., of the Q2, and Q3 peaks in each sample.

Deconvoluted Peak Area				
	Q2	Q3	Q4	Q2/(Q2+Q3)
401	1.26E+08	5.19E+08	1.66E+08	19.48%
405	6.70E+06	1.57E+08	8.04E+08	4.09%
bare	1.06E+06	3.81E+06	1.50E+06	21.77%

Table 11. Chart comparing the peak areas and Q2/Q3 ratios for samples 401, 405 and the bare sample.

The proportions of the Q2 and Q3 peaks are similar for the bare sample and 401. For sample 405, the Q2 peak is much smaller, compared to the Q3 peak, than in the other two samples. This analysis does not give a definite proportion for geminal hydroxyl groups in the sample, but it does demonstrate that the proportion of geminal hydroxyl groups is lowest in sample 405. In a similar vein, Table 12 shows the proportion of single Q3 silanol peaks compared to the bulk Q4

Deconvoluted Peak Area				
	Q2	Q3	Q4	Q3/(Q3+Q4)
401	1.26E+08	5.19E+08	1.66E+08	7.57E-01
405	6.70E+06	1.57E+08	8.04E+08	1.64E-01
bare	1.06E+06	3.81E+06	1.50E+06	7.17E-01

Table 12. Chart comparing the peak areas and Q3/Q4 ratios for sample 401, 405, and the bare sample.

siloxane peaks. Sample 405 appears to have a lower proportion of single Q3 silanol groups, in relation to Q4 siloxane groups, than either 401 or the bare sample. Sample 401 appears to have a slightly higher proportion of single Q3 silanol groups, compared to Q4 siloxane groups, than the bare sample. This is simply a quantification of the relationships seen in Figure 24. Overall, sample 405 has been shown to be greatly influenced by high pH chemistry through the results of both NMR and TGA analysis. Concurrently, sample 401 has been shown to have a larger amount of surface hydroxyl groups than either 405 or the bare sample by both NMR and TGA characterization techniques.

Conclusions

CAB-O-SIL based cryogel samples have been shown to exhibit morphological and chemical characteristics that differ from the plain CAB-O-SIL nanoparticulate silica. Freezing and freeze drying create a powder that is macroscopically distinct, in terms of morphology, from air dried samples, with each having a higher bulk density than the bare silica. Freezing and freeze drying do not result in evacuation of a higher proportion of hydrogen bonded hydroxyl groups during TGA. While higher bulk density could result in more interaction between surface groups of different primary nanoparticles, hydrogen bonding with water molecules may preclude much of this direct interaction. In all cases, excepting the heated sample 407, cryogel samples exhibited a higher weight loss from 200-600°C than the bare silica. This indicates that most cryogel samples contain a larger amount of hydrogen bonded hydroxyl than the bare sample. However, the greater hydroxyl content of the cryogel surfaces seems to be due to the immersion in excess water rather than any other processing parameters. Freezing and freeze drying *have* been shown to have an effect on the morphological properties of cryogel powders, such as bulk density and pore volume. Cryogel samples re-immersed in water and air dried do not exhibit a

drastic change in macroscopic appearance, indicating some type of permanence to the changes in post-processing particle morphology. NMR results confirmed sample 401 contains slightly more single silanol groups than the bare sample (Table 12). The NMR analysis showing reduced hydroxyl content in sample 405 makes sense considering the reduced surface area of the sample. However, TGA data seems to indicate that sample 405 has a similar amount of hydroxyl groups compared to other cryogel samples. The strange nature of sample 405 is likely entirely due to the adjustment of its initial aqueous slurry to pH 10. This adjustment resulted in a decrease in surface area, caused by dissolution and redeposition of silica at high pH, and some degree of silanol condensation, likely between hydroxyl groups on different primary particles.

References

[1]Iler, Ralph K. *The Chemistry of Silica,* John Wiley and Sons: New York, 1979.

[2]Skuja, L., et al. "Defects in oxide glasses." *physica status solidi (c)* 2.1 (2005): 15-24.

[3]Sigma Aldrich. (2014). *Fumed Silica: Product Information (S 5130).* Retrieved from http://www.sigmaaldrich.com/content/dam/sigma-aldrich/docs/Aldrich/Product_Information_Sheet/s5130pis.pdf

[4]Cabot Corporation (2014). *Overview of CAB-O-SIL® Untreated Fumed Silicas.* Retrieved from http://www.cabot-corp.com/Silicas-And-Aluminas/Adhesives-and-Sealants/Product-Information/GN200808261330PM9120/, 15 July, 2014

[5]Zhuravlev, L. T. "The surface chemistry of amorphous silica. Zhuravlev model."*Colloids and Surfaces A: Physicochemical and Engineering Aspects* 173.1 (2000): 1-38.

[6]Blitz, Jonathan P. "Reactions of titanium tetrachloride with modified silica gel surfaces studied by diffuse reflectance FT-IR spectroscopy." *Colloids and surfaces* 63.1 (1992): 11-19.

[7]Gun'ko, Vladimir M., Irina N. Savina, and Sergey V. Mikhalovsky. "Cryogels: Morphological, Structural and Adsorption characterisation." *Advances in colloid and interface science* 187 (2013): 1-46.

[8]Gun'ko, V. M., et al. "High-Pressure Cryogelation of Nanosilica and Surface Properties of Cryosilicas." *Colloids and Surfaces A: Physicochemical and Engineering Aspects* 436 (2013): 618-632.

[9]Nishihara, Hirotomo, et al. "Preparation of titania–silica cryogels with controlled shapes and photocatalysis through unidirectional freezing." *Materials Letters* 64.8 (2010): 959-961.

[10]Wang, Xu, et al. "Cryogel synthesis of hierarchical interconnected macro-/mesoporous Co_3O_4 with superb electrochemical energy storage." *The Journal of Physical Chemistry C* 116.7 (2012): 4930-4935.

[11]Mirabella, Francis M. *Modern techniques in applied molecular spectroscopy*. John Wiley and Sons: New York, 1998.

[12]Gun'ko, V. M., et al. "High-Pressure Cryogelation of Nanosilica and Surface Properties of Cryosilicas." *Colloids and Surfaces A: Physicochemical and Engineering Aspects* 436 (2013): 618-632.

[13]Kingery, W. D., H. K. Bowen, and D. R. Uhlmann. "Introduction to ceramics, 1976." *New York*: 788-1016.

[14]Larkiri, Danny E. "Compositional Analysis by Thermogravimetry: The Development of a Standard Method." *Compositional Analysis by Thermogravimetry* 997 (1988): 28.

[15]Barrett, Elliott P., Leslie G. Joyner, and Paul P. Halenda. "The determination of pore volume and area distributions in porous substances. I. Computations from nitrogen isotherms." *Journal of the American Chemical society* 73.1 (1951): 373-380.

[16]Brunauer, Stephen, Paul Hugh Emmett, and Edward Teller. "Adsorption of gases in multimolecular layers." *Journal of the American Chemical Society* 60.2 (1938): 309-319.

[17]Leonardelli, S., et al. "Silicon-29 NMR study of silica." *Journal of the American Chemical Society* 114.16 (1992): 6412-6418.

[18]Liu, Changhua C., and Gary E. Maciel. "The fumed silica surface: A study by NMR." *Journal of the American Chemical Society* 118.21 (1996): 5103-5119.

[19]S.J. Gregg, K.S.W. Sing, Adsorption, Surface Area and Porosity, Academic Press, London, 1982.

[20]V. M. Gun'ko, Consideration of the multicomponent nature of adsorbents during analysis of their structural and energy parameters, Theoret. Experim. Chem. 36 (2000) 319-324.

[21]Brinker, C. J. "Hydrolysis and condensation of silicates: effects on structure."*Journal of Non-Crystalline Solids* 100.1 (1988): 31-50.

[22]Pramanik, A., et al. "A mechanistic study of the initial stage of the sintering of sol-gel derived silica nanoparticles." *International Journal of Modern Engineering Research (IJMER)* Vol.3, Issue.2, March-April. 2013 pp-1066-1070

[23]Brinker, C. J., and S. P. Mukherjee. "Conversion of monolithic gels to glasses in a multicomponent silicate glass system." *Journal of Materials Science* 16.7 (1981): 1980-1988.

[24]Kosmulski, Marek. *Chemical properties of material surfaces*. CRC press, 2001.

[25]Morrow, B. A., and A. J. McFarlan. "Surface vibrational modes of silanol groups on silica." *The Journal of Physical Chemistry* 96.3 (1992): 1395-1400.

[26]Cabot Corporation (2014). *Fumed Silica and Fumed Alumina in Coatings Applications*. Retrieved from http://www.cabot-corp.com/wcm/download/en-us/fs/FS%20&%20FA%20in%20Coatings%20086769-eng.pdf, 23 October, 2014

[27]Armistead, C. G., et al. "Surface hydroxylation of silica." *The Journal of Physical Chemistry* 73.11 (1969): 3947-3953.

[28]Pohl, E. R., and F. D. Osterholtz. "Kinetics and mechanism of condensation of alkylsilanols in aqueous solution." *Silanes, Surfaces, and Interfaces* (1986): 481-500.